Anisomycin downregulates gap-junctional intercellular communication via the p38 MAP-kinase pathway

Takahiko Ogawa[1,*], Tomonori Hayashi[1], Seishi Kyoizumi[1], Yoichiro Kusunoki[1], Kei Nakachi[1], Donald G. MacPhee[1], James E. Trosko[2], Katsuko Kataoka[3] and Noriaki Yorioka[4]

[1]Department of Radiobiology and Molecular Epidemiology, Radiation Effects Research Foundation, Hiroshima, Japan
[2]National Food Safety Toxicology Center, Department of Pediatrics/Human Development, Michigan State University, East Lansing, MI, USA
[3]Department of Histology and Cell Biology, Graduate School of Biomedical Sciences, Hiroshima University, Hiroshima, Japan
[4]Department of Molecular and Internal Medicine, Graduate School of Biomedical Sciences, Hiroshima University, Hiroshima, Japan
*Author for correspondence (e-mail: tk-ogawa@hph.pref.hiroshima.jp)

Accepted 11 December 2003
Journal of Cell Science 117, 2087-2096 Published by The Company of Biologists 2004
doi:10.1242/jcs.01056

Summary

Phosphorylation of connexin 43 (Cx43) molecules (e.g. by extracellular signal-regulated kinase) leads to reductions in gap-junctional intercellular communication (GJIC). GJIC levels also appear to be lower in the presence of p38 mitogen-activated protein (MAP) kinase, for unknown reasons. In this study, we used assays of the recovery of fluorescence by photobleached WB-F344 cells to demonstrate that GJIC levels are decreased by anisomycin [a protein synthesis inhibitor as well as an activator of p38 MAP kinase and c-Jun N-terminal kinases (JNK)] as a result of time-dependent depletion of the phosphorylated forms of Cx43. Using immunohistochemistry, we also detected far less of the Cx43 proteins at cell borders. These findings agree with the photobleaching assay results. Moreover, prior treatment with SB203580 (a specific inhibitor of p38 MAP kinase) appeared to be effective in preventing the loss of phosphorylated forms of Cx43 and the loss of Cx43 proteins at cell borders. Total protein labelling with [^{35}S]-methionine and [^{32}P]-orthophosphates labelling of Cx43 showed that anisomycin enhanced the phosphorylation level of Cx43 along with inhibition of protein synthesis. SB203580 prevented the former but not the latter. The effect of anisomycin on GJIC was not dependent on the inhibition of protein synthesis because the addition of SB203580 completely maintained the level of GJIC without restoring protein synthesis. The Cx43 phosphorylation level increased by anisomycin treatment, whereas the amount of phosphorylated forms of Cx43 decreased, suggesting that activation of Cx43 phosphorylation might lead to the loss of Cx43. These results suggest that activation of p38 MAP kinase leads to reduction in the levels of phosphorylated forms of Cx43, possibly owing to accelerated degradation, and that these losses might be responsible for the reduction in numbers of gap junctions and in GJIC.

Key words: p38 MAP kinase, Connexin 43, GJIC, Anisomycin, SB203580, Protein synthesis inhibition

Introduction

Gap junctions consist of plasma-membrane-spanning channels that permit the intercellular exchange of ions and low molecular weight molecules (Loewenstein, 1990). Gap-junctional intercellular communication (GJIC) is therefore believed to be involved in cell growth and differentiation; aberrant control might also play an important role in cancer development (Loewenstein, 1990; Trosko and Ruch, 1998). The mechanisms that regulate GJIC are not yet fully understood, although there is evidence that post-translational alterations of the connexins are involved (Musil and Goodenough, 1991; Musil and Goodenough, 1993; Trosko and Ruch, 1998). Connexin 43 (Cx43) is a widely expressed gap-junction protein found in many animal organs (Beyer et al., 1987; Dupont et al., 1991) and many recent investigations into the relationships between Cx43 phosphorylation and events in gap-junction assembly (channel gating) suggest that several protein kinases are capable of mediating both Cx43 phosphorylation and GJIC inhibition (Berthoud et al., 1993; Cho et al., 2002; Hossain et al., 1998a; Kanemitsu and Lau, 1993; Laird et al., 1995; Lau et al., 1992; Musil et al., 1990; Musil and Goodenough, 1991; Musil and Goodenough, 1993; Trosko and Ruch, 1998; Warn-Cramer et al., 1998; Warn-Cramer et al., 1996).

The mitogen-activated protein (MAP) kinase belongs to an important family of protein kinases that act by phosphorylating specific amino acids on their target substrates. Of the classic MAP kinases, extracellular signal-regulated protein kinases 1 and 2 (ERK) are especially well known and can be activated by various physiological stimuli, including some growth factors (Seger and Krebs, 1995). Previous investigations have shown that activation of ERK is an important element in the regulation of both GJIC and Cx43 (Berthoud et al., 1993; Hossain et al., 1998b; Hossain et al., 1999a; Kanemitsu and Lau, 1993; Lau et al., 1992; Ruch et al., 2001; Warn-Cramer et al., 1996; Warn-Cramer et al., 1998) but other studies investigating a range of ERK activators and inhibitors suggest that the correlation between ERK activation, Cx43 phosphorylation and GJIC

inhibition is by no means perfect (Hii et al., 1995a; Hii et al., 1995b; Hossain et al., 1998a; Hossain et al., 1999a). Previous evidence (Hii et al., 1995b; Matesic et al., 1994) indicates that Cx43 hyperphosphorylation by ERK activation, as indicated by a reduction in the mobility [on sodium dodecyl sulfate (SDS) gels] of the resulting Cx43 derivatives, is one mechanism of GJIC disruption available to cells, but it seems likely that other mechanisms of disruption, not necessarily dependent on Cx43 hyperphosphorylation, can and do exist.

We believe that other kinases and/or cofactors might be involved in the process of GJIC disruption; it is even possible that GJIC blockage is dependent upon the coordinated action of different MAP kinases, including ERK. Other members of the MAP-kinase family might also be involved (Cano and Mahadevan, 1995). Of these, p38 MAP kinase is the most obvious candidate, if only because of its involvement in signal transduction pathways that work in parallel with ERK (with which it shares ~50% sequence identity) (Tong et al., 1997). Given that these two signal transduction pathways overlap and 'cross talk' (Cano and Mahadevan, 1995; Helliwell et al., 2000; Töröcsik and Szeberényi, 2000), it seems reasonable to postulate a role for both p38 MAP kinase and ERK in the downregulation of Cx43 and/or the disruption of GJIC. Two recent reports, one suggesting that p38 MAP kinase is involved in GJIC upregulation and a second suggesting its involvement in GJIC downregulation (Cho et al., 2002; Polontchouk et al., 2002), are difficult to interpret because different cell types were used. Such contradictory findings do little if anything to clarify the relationship between p38 MAP kinase and GJIC regulation, and we thus designed a new study that we hoped would allow us to determine whether p38 MAP kinase contributes to Cx43 phosphorylation and/or gap-junctional disruption and, if so, how.

As a first step, we decided to examine the effects of anisomycin on GJIC. This interesting compound is well known to act as a protein synthesis inhibitor and a pharmacologically specific activator of two distinct kinds of kinases, p38 MAP kinase and c-Jun N-terminal kinases (JNKs) (Barros et al., 1997; Cano et al., 1994; Cano and Mahadevan, 1995; Hazzalin et al., 1998; Kyriakis et al., 1994), both of which can be stimulated by a wide variety of stress stimuli, including DNA damage, heat and osmotic shock, cytokines, and protein synthesis inhibitors (Minden and Karin, 1997). We also designed experiments in which we made use of a specific inhibitor of p38 MAP kinase, known as SB203580 (Cuenda et al., 1995; Tong et al., 1997), and other kinds of cell-to-cell-junction-related proteins, including ZO-1, occludin, E-cadherin and β-catenin. We also performed total cell metabolic labelling with [^{35}S]-methionine in order to try and rule out any possibility that the observed effects of anisomycin resulted from activation of the JNK pathway or a more general inhibitory effect on protein synthesis. Our findings strongly favour the hypothesis that p38 MAP kinase plays an important role in the disruption of GJIC by reducing the total amounts of phosphorylated Cx43, which effect is possibly due to accelerated degradation of phosphorylated Cx43 in the cells, and reducing the number of Cx43 proteins observed at cellular borders.

Materials and Methods

Cell culture

The Fisher 344 rat-liver-derived epithelial cell line WB-F344 (Tsao et al., 1984) was cultured at 37°C in a 95% O_2, 5% CO_2 atmosphere in a modified Eagle's medium (MEM) supplemented with 7% foetal calf serum (FCS), 50 U ml^{-1} penicillin and 50 μg ml^{-1} streptomycin sulfate. Passage 8-21 cells were used in all experiments.

Materials

Anisomycin (2-*p*-methoxyphenylmethyl-3-acetoxy-4-hydroxy-pyrrolidine) and dimethyl sulfoxide (the vehicle for SB203580) were from Sigma (St Louis, MO) and SB203580 [4-(4-fluorophenyl)-2-(4-methylsulphonylphenyl)-5-(4-pyridyl) imidazole] was from Calbiochem (La Jolla, CA). PhosphoPlus p38 MAP kinase and SAPK/JNK Antibody Kit™ were from Cell Signaling Technology (Beverly, MA). Carboxyfluorescein diacetate (CFDA) was from Molecular Probes (Eugene, OR). Lab-Tek Chamber Slides™ were from Nalge Nunc International (Naperville, IL). Anti-Cx43 monoclonal antibody and Alexa-488-conjugated goat anti-mouse antibody were from Chemicon International (Temecula, CA) and Molecular Probes (Eugene, OR), respectively. Anti-ZO-1 and anti-occludin polyclonal antibodies (Zymed Laboratories, San Francisco, CA), and anti-E-cadherin (Transduction Laboratories, Lexington, KY), anti-β-catenin (Zymed Laboratories), anti-β-actin (Sigma) monoclonal antibodies were also used. SDS polyacrylamide-gel electrophoresis (SDS-PAGE) supplies and reagents for western blot analyses were from Bio-Rad (Richmond, CA). The enhanced chemiluminescence detection kit was from Renaissance Western Blot Chemiluminescence Reagent (NEN Life Science Products, Boston, MA). [^{35}S]-Methionine and [^{32}P]-orthophosphates were from Perkin Elmer Life and Analytical Sciences (Boston, MA).

Cell treatments with anisomycin and SB203580

WB-F344 cells seeded in dishes or slides were grown to approximately 80% confluence. The medium was replaced with fresh medium containing 0.2% FCS and the cells were then incubated for a further 48 hours. Cells were treated with 10 μg ml^{-1} (10 mg ml^{-1} stock in distilled water) anisomycin for 5, 30 60, 90, 120 and 180 minutes at 37°C. To block the p38 MAP kinase, cells were treated with 10 μM SB203580 (50 mM stock in dimethyl sulfoxide) for 30 minutes at 37°C before being exposed to anisomycin for 60 minutes. Controls for the experiments were treated with 0.02% dimethyl sulfoxide and/or distilled water. Aliquots of the treated cell suspensions were then used for measurements of GJIC, MAP kinase activation levels, Cx43 phosphorylation levels and immunofluorescence.

FRAP assay for GJIC

Our procedure was a modified version of the standard method for measuring GJIC by quantitative fluorescence recovery after photobleaching (FRAP) (Ogawa et al., 1999; Trosko et al., 2000; Wade et al., 1986). Assays were performed using an ACAS Ultima laser cytometer (Meridian Instruments, Okemos, MI). After selectively bleaching cells with a micro-laser beam, we followed the rate of transfer of CFDA from adjacent labelled cells back into bleached cells. Recovery of fluorescence was assessed at 1-minute intervals and recovery rates (RRs) were calculated as percentages of fluorescence recovered per minute. Anisomycin and/or SB203580 were not present in the medium during labelling of the cells with CFDA, photobleaching or calculation of RR. All calculated rates were corrected for the loss of fluorescence by unbleached control cells and the results expressed as the average percentage (mean±s.e.m.) recovery rate of treated cells relative to the recovery rate of untreated cells.

Indirect immunofluorescence and confocal microscopy

WB-F344 cells were cultured as previously described (Trosko et al.,

2000) and the cells plated on a Lab-Tek Chamber Slide™ for anisomycin and/or SB203580 treatment. After treatment, the cells were washed twice in PBS and fixed in periodate-lysine-paraformaldehyde fixative for 30 minutes; they were then washed and permeabilized three times with 0.1% Triton-X-100/PBS (PBST), and incubated in 20% BlokAce (Dainihon Pharmaceuticals, Tokyo, Japan) for 1 hour. The next stage involved overnight incubation at 4°C in a 1:2000 dilution of anti-Cx43 monoclonal antibody (Chemicon) followed by three washes with PBST before incubation in Alexa-488-conjugated goat anti-mouse antibody (Molecular Probes) at a dilution of 1:2000 for 1 hour in dark conditions. The cells were then washed three times in PBST and once in PBS before being mounted in Gel/Mount (Biomeda, Foster City, CA) for examination in a Zeiss LSM 510 laser-scanning confocal microscope.

Immunoblotting

Cells grown to approximately 80% confluence in 10-cm dishes were treated with anisomycin, anisomycin plus SB203580, or SB203580 plus either distilled water or dimethyl sulfoxide as the vehicle control. At the end of the treatment period, the monolayers were rinsed three times with ice-cold PBS. Lysates were prepared with ice-cold lysis buffer containing 20 mM Tris-buffered saline (TBS), pH 7.5, 1% Triton X-100, 150 mM NaCl, 1 mM each of EDTA, EGTA, β-glycerophosphate, Na_3VO_4 and phenylmethyl-sulfonyl fluoride (PMSF), 2.5 mM sodium pyrophosphate, and 1 μM leupeptin, and then sonicated. The samples were diluted 1:5 in water and their protein concentrations determined using the DC protein assay™ (Bio-Rad). Samples (20 μg) of protein were then dissolved in Laemmli sample buffer, separated on 12.5% polyacrylamide gels, and transferred to polyvinilidene difluoride membranes (Bio-Rad) before determining their phosphorylated p38 MAP kinase and JNK levels according to the manufacturer's protocols for PhosphoPlus p38 (Thr180/Tyr182) and SAPK/JNK (Thr183/Tyr185) MAP Kinase Antibody Kit™ (Cell Signaling Technology) assays. The Cx43 content of the various samples was also determined by incubating the samples with an anti-Cx43 monoclonal antibody (Chemicon; diluted 1:2000), and later adding a horseradish-peroxidase-conjugated secondary antibody (diluted 1:2000; Amersham, Arlington Heights, IL) and an enhanced chemiluminesce detection reagent (NEN Life Science Products). The membrane was stripped and reprobed with anti-ZO-1 and anti-occludin polyclonal antibodies (Zymed, diluted 1:2000), and anti-E-cadherin (Transduction, 1:2000), anti-β-catenin (Zymed, 1:2000) and anti-β-actin (Sigma, 1:2000) monoclonal antibodies, respectively. The average control value was assigned an arbitrary value of 1 unit and relative band intensities were standardized to this arbitrary unit (AU).

[^{35}S]-Methionine total protein metabolic labelling of WB-F344 cultures

To confirm that anisomycin acts as a protein synthesis inhibitor in vivo, metabolic labelling of WB-F344 cells was conducted. Cells were starved of methionine for 30 minutes at 37°C in methionine-free MEM. The medium was then replaced with fresh labelling medium containing [^{35}S]-methionine (0.1 mCi per 6 cm dish of cells) and incubation was continued for the final 60 minutes. Anisomycin and SB203580 were incubated for the last 60 or 90 minutes. The radioactive medium was removed after a pulse labelling and cells were rinsed with PBS and solubilized in cold RIPA buffer containing 2 mM sodium orthovanadate, 1 mM PMSF and 1% Triton-X-100. Cells were harvested and the DNA was sheared by drawing the lysate through a 26 G needle. After centrifugation, supernatant was collected and resuspended (1 μl) in 1 ml of scintillate followed by liquid scintillation spectrometry.

[^{32}P]-Orthophophate metabolic labelling of WB-F344 cultures

Radioimmunoprecipitation of Cx43 was performed as described above. Cells were starved of phosphates for 30 minutes at 37°C in phosphate-free MEM and supplemented with 0.2% dialysed FCS. The medium was then replaced with fresh labelling medium containing [^{32}P]-orthophosphate (0.1 mCi per 6 cm dish of cells) and preincubation was continued for 60 minutes. After the addition

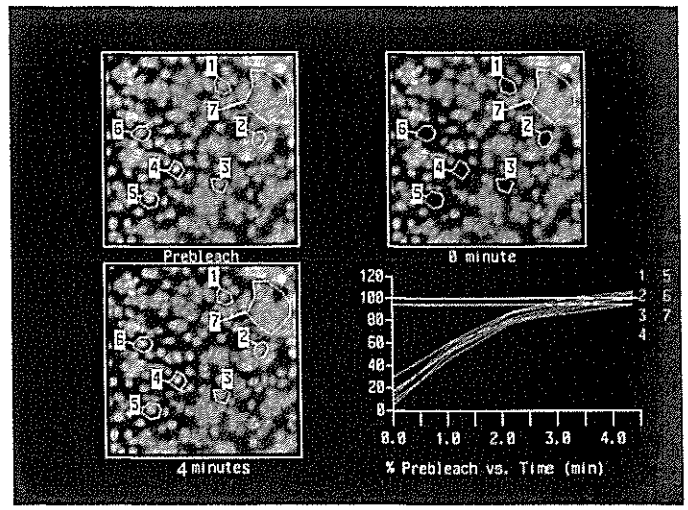

control

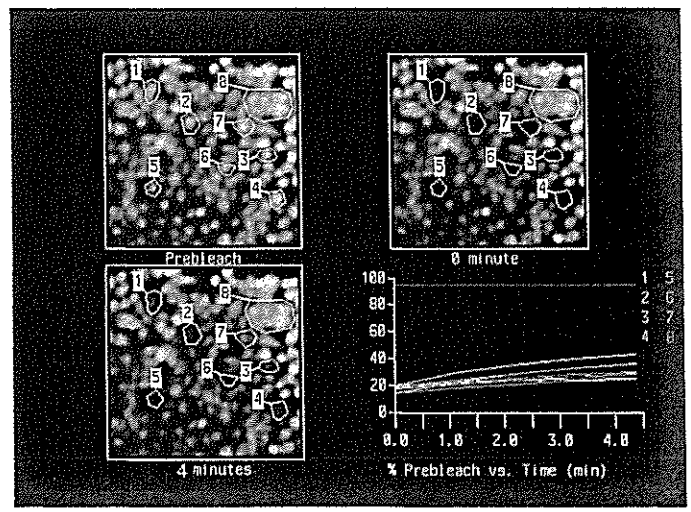

anisomycin

Fig. 1. Typical digitized fluorescence images and plots of fluorescence recovery after photobleaching. With (anisomycin) or without (control) anisomycin treatment for 60 minutes, cells were labelled with 5,6-carboxyfluorescein diacetate. Suitable fields of cells were identified using a 40× objective lens. Such fields contained many cells that were in contact with each other but not too confluent. Each field was scanned to generate a digital image of fluorescence (Prebleach). After the initial scan, selected cells were photobleached (0 minute, numbers 1-6). Sequential scans were then carried out at 30 second intervals to detect recovery of fluorescence in the bleached cells (4 minute, numbers 1-6). Images were digitally recorded for analysis. Several unbleached cells were also monitored to provide control data (number 7). Typical plots of fluorescence recovery after photobleaching are shown (proportion of prebleaching against time). A rising slope indicates the recovery of fluorescence. The percentage recovery of fluorescence over time was determined for each selected cell and the data were corrected for the background loss of fluorescence in one area (number 7).

of anisomycin and/or SB203580, culture was continued in radioactive medium. Each treatment group was exposed to 0.02% dimethyl sulfoxide as vehicle alone for 90 minutes, anisomycin at 10 μg ml^{-1} for 60 minutes, SB203580 plus anisomycin (pretreatment of SB203580 for 30 minutes, then co-treatment with anisomycin for an additional 60 minutes), or SB203580 alone for 90 minutes. Anisomycin and SB203580 were incubated for the last 60 or 90 minutes. The radioactive medium was removed after one pulse for three hours, and cells were rinsed with TBS and solubilized in cold RIPA buffer containing sodium orthovanadate (2 mM), 1 mM PMSF and 1% Triton-X-100. Cellular debris was concentrated by centrifugation (10 minutes, 20,400 *g*), and supernatant was collected and incubated with 20 μl of a 50% slurry of Protein-G/Sepharose CL-4B (Amersham Pharmacia Biotech, Uppsala, Sweden) and the samples were rotated for 1 hour at room temperature. The samples were then centrifuged at 20,400 *g* for 10 minutes and the supernatant was collected and incubated with 1 μg anti-Cx43 monoclonal antibody (Chemicon) for 1 hour, followed by addition of 20 μl of the 50% slurry of Protein-G/Sepharose CL-4B for 1 hour. The immunoprecipitates were washed four times with TBS and supplemented with Laemli sample buffer and boiled at 95°C for 5 minutes. Samples, derived from equal volume of cell lysates, were electrophoresed on 12.5% SDS gels and autoradiographed. Phosphorylated bands were analysed by autoradiography using Personal.Molecular Imager FX (Bio-Rad).

Densitometric analysis

Exposed films were scanned using a flatbed scanner and band density was analysed using NIH Image™.

Statistical analysis

Data were analysed using Statview II software™ (Apple Computer, Cupertino, CA). The two-tailed unpaired Student's *t*-test was used in comparisons of the anisomycin- or SB203580-treated cultures with control cultures; differences were considered significant at $P<0.05$. Results are expressed as the mean±s.e.m.

Results

Typical digitized fluorescence images and plots of fluorescence recovery after photobleaching of untreated cells and cells treated with anisomycin for 60 minutes are shown in Fig. 1. The untreated cells recovered their fluorescence within 4 minutes, whereas the anisomycin treated cells did not.

To determine whether this anisomycin-induced effect is specifically related to the ability of anisomycin to activate p38 MAP kinase, we also examined the phosphorylation status of the other MAP kinase families. To do this, we assessed the activities of p38 MAP kinase and JNK by measuring the levels of their active phosphorylated forms using immunoblotting. Densitometric band analyses of the phosphorylated forms of p38 MAP kinase and JNK (p46/p54) are shown in Fig. 2. The time-course study shows that anisomycin treatment led to the phosphorylation of both p38 MAP kinase and JNK (Fig. 2A). Phosphorylation of p38 MAP kinase was not observed in the absence of anisomycin, a peak level being reached at 5 minutes and sustained until 60 minutes. Phosphorylated JNK levels increased much more slowly after anisomycin treatment, with a peak becoming evident at 30 minutes. The dose study shows that phosphorylated p38 MAP kinase and JNK increased at concentrations of more than 0.1 μg ml^{-1}, with peaks of 8.1 times the control at 10 μg ml^{-1} (p38 MAP kinase) and 8.3 times the control at 1 μg ml^{-1} (JNK) (Fig. 2B).

We therefore used the FRAP assay to measure the RR at each time point as a simple way of quantifying the effects of anisomycin treatment on GJIC. The results were consistent: the addition of anisomycin (10 μg ml^{-1}) to WB-F344 cells led to a time-dependent decrease in RR, in that there was a significant decrease to ~80% of the control value at 5 minutes and then to ~55% at 30 minutes and ~50% at 60 minutes (this was the lowest level reached and was retained up to 180 minutes) (Fig. 3A). Cells that had been incubated for up to 60 minutes with the same concentration of anisomycin turned out to have near-normal RRs only 24 hours after the removal of the anisomycin (data not shown). To assess the dose effect of anisomycin, 60 minute assays were performed at various concentrations of anisomycin. There was no significant decrease at <0.1 μg ml^{-1} but the RR decreased to about 75% of control at 1 μg ml^{-1}, with

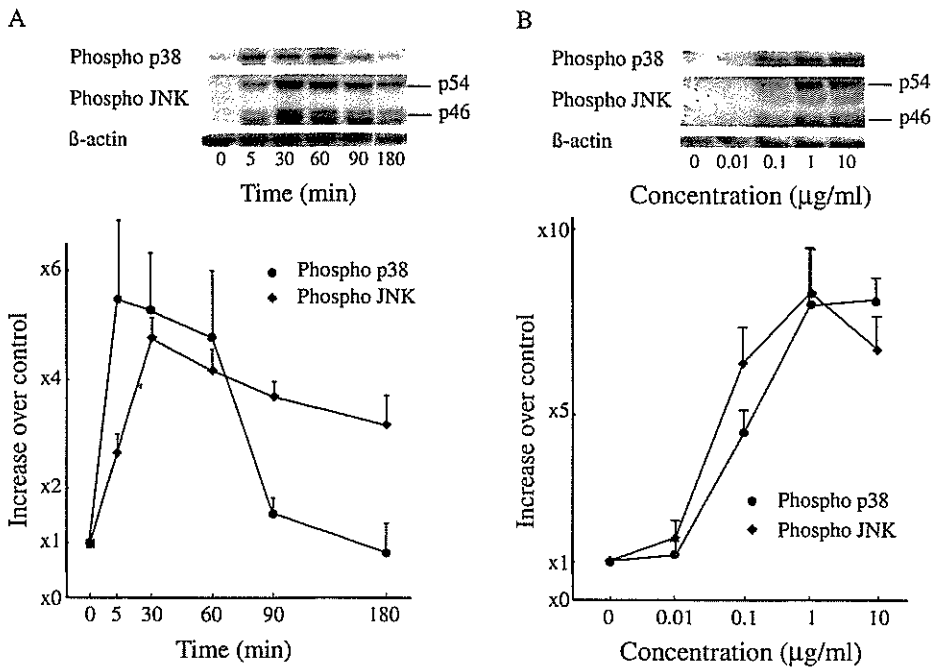

Fig. 2. Time (A) and dose (B) course analyses of the effect of anisomycin on MAP kinase activity. After treatment with anisomycin, cell lysates were prepared and 20 μg protein was separated on 12.5% gel and transferred onto a PVDF membrane. The same membrane was probed and reprobed after stripping with antibodies against doubly phosphorylated p38 MAP kinase, phosphorylated p46/p54 and β-actin as control in protein loading. These results were representative of three experiments, each performed with a different preparation of cells, and are expressed as the fold activity (means±s.e.m.) of band density relative to that of untreated control by densitometric analysis.

maximal effect at 10 μg ml^{-1} (about 40% of control) (Fig. 3B). In order to assess effects of anisomycin concentrations on protein synthesis, we estimated the amount of proteins produced de novo using an [^{35}S]-methionine metabolic labelling assay (Fig. 3C). There was a significant decrease in the total protein level even at the lowest concentration (10 ng ml^{-1}) of anisomycin by which p38 MAP kinase could not be activated (Fig. 2B). Thus, we could not dissociate the inhibition of protein synthesis from the GJIC downregulation by using

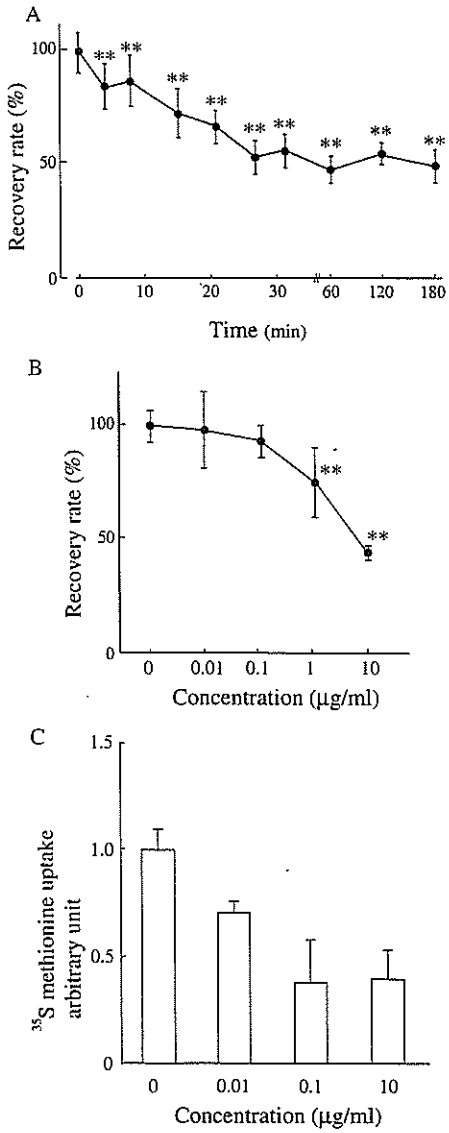

Fig. 3. Time (A) and dose (B) course analyses of the effect of anisomycin on GJIC. GJIC was estimated by FRAP in cells treated with anisomycin. Results are expressed as the percentage (mean±s.e.m.) of RR relative to that of control cells (set to 100%) treated with distilled water. These results are representative of at least three experiments. $^{**}P<0.01$ versus cells incubated with control. (C) To examine the effect of anisomycin as protein synthesis inhibitor, we used a [^{35}S]-methionine metabolic labelling assay. At each concentration (0.01 μg ml^{-1}, 0.1 μg ml^{-1} and 10 μg ml^{-1}) of anisomycin, [^{35}S]-labelled protein level was shown as radioactivity by liquid scintillation spectrometry. For comparison, the radioactivity of control was arbitrarily set at 1. Results were expressed as means±s.e.m. of three separate experiments.

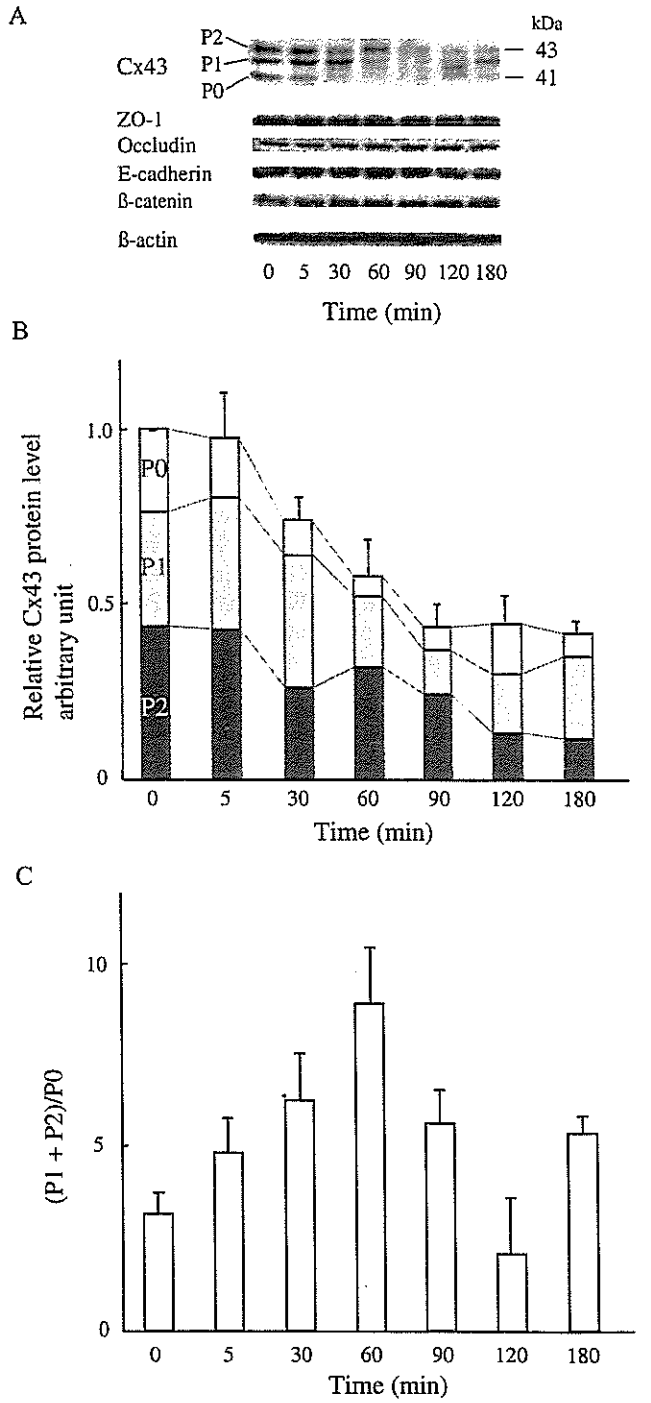

Fig. 4. Phosphorylation of Cx43 protein in anisomycin-treated cells. (A) Typical western blots of the Cx43 protein, with ZO-1, occludin, E-cadherin and β-catenin as reference proteins and β-actin as a control for protein loading. Numbers indicate the time from the addition of anisomycin. After incubation with anisomycin (10 μg ml^{-1}) for 5, 30, 60, 90, 120 and 180 minutes, whole-cell extracts (20 μg per lane) were probed with antibodies. All samples show multiple Cx43 protein bands (P0, P1 and P2) depending on the phosphorylation level, and equal levels of reference proteins. (B) Densitometric analysis of the most important bands of Cx43 protein. The relative band intensities are shown. For assessment of each protein, the total amounts of control were arbitrarily set at 1. (C) Each column displays the ratio of (P1+P2):P0. Values are the means±s.e.m. of three separate experiments.

lower concentrations of anisomycin (around 25-50 ng ml^{-1}; so-called subinhibitory level) that appeared to have an ability to activate the p38 MAP kinase.

An examination of the profiles of the various forms of Cx43 before and after anisomycin treatment led to some interesting findings. Before treatment, we could detect three predominant forms of the Cx43 protein by SDS-PAGE; each form could be seen as a distinct immunoreactive band of between 41 and 43 kDa. The minor unphosphorylated form of Cx43 (P0) migrated fastest, whereas the more abundant phosphorylated forms (P1 and P2) migrated more slowly (Fig. 4A), as noted previously (Trosko and Ruch, 1998). After setting the total Cx43 level of control cells at 1 AU, we noted that the combined intensities of P0, P1 and P2 had reached their lowest point (0.46 AU) at 90 minutes and retained up to 180 minutes. Following the addition of anisomycin, the absolute amount of the phosphorylated forms of Cx43 (i.e. P1+P2), and also of P0, tended to decrease time dependently until 120 minutes, which coincided almost precisely with the disruption of GJIC (Fig. 3A). By contrast, none of ZO-1, occludin, E-cadherin and β-catenin showed any changes. The ratios of P1+P2 to P0 were assayed at intervals throughout the course of a 180-minute treatment period. Although the ratio increased about ninefold, reaching a peak at 60 minutes, it then decreased rapidly, only to increase again at 180 minutes (Fig. 4C). The disruption of GJIC that we were observing appeared to vary inversely with the absolute amounts of Cx43 phosphorylated forms P1+P2 and P0 that were present.

As expected, we were able to detect phosphorylation of p38 MAP kinase in anisomycin-treated cells not pretreated with SB203580, whereas cells treated with only SB203580 did not appear to contain any phosphorylated p38 MAP kinase whatsoever (Fig. 5A). The levels of p38 MAP kinase phosphorylation in normal cells were found to have increased about sixfold after anisomycin treatment, but only twofold or so in cells pretreated with SB203580 (Fig. 5B). Anisomycin treatment also led to significant increases (about fivefold) in JNK phosphorylation levels in normal cells. Although pretreatment with SB203580 led to somewhat smaller anisomycin-induced increases (about fourfold), there was every indication that SB203580 was far less effective at blocking JNK phosphorylation than it had been at blocking p38 MAP kinase phosphorylation. We found that cells pretreated with 10 μM SB203580 for 30 minutes were no longer subject to the anisomycin-induced reductions in GJIC experienced by cells pretreated with SB203580-free medium (Fig. 5C). To

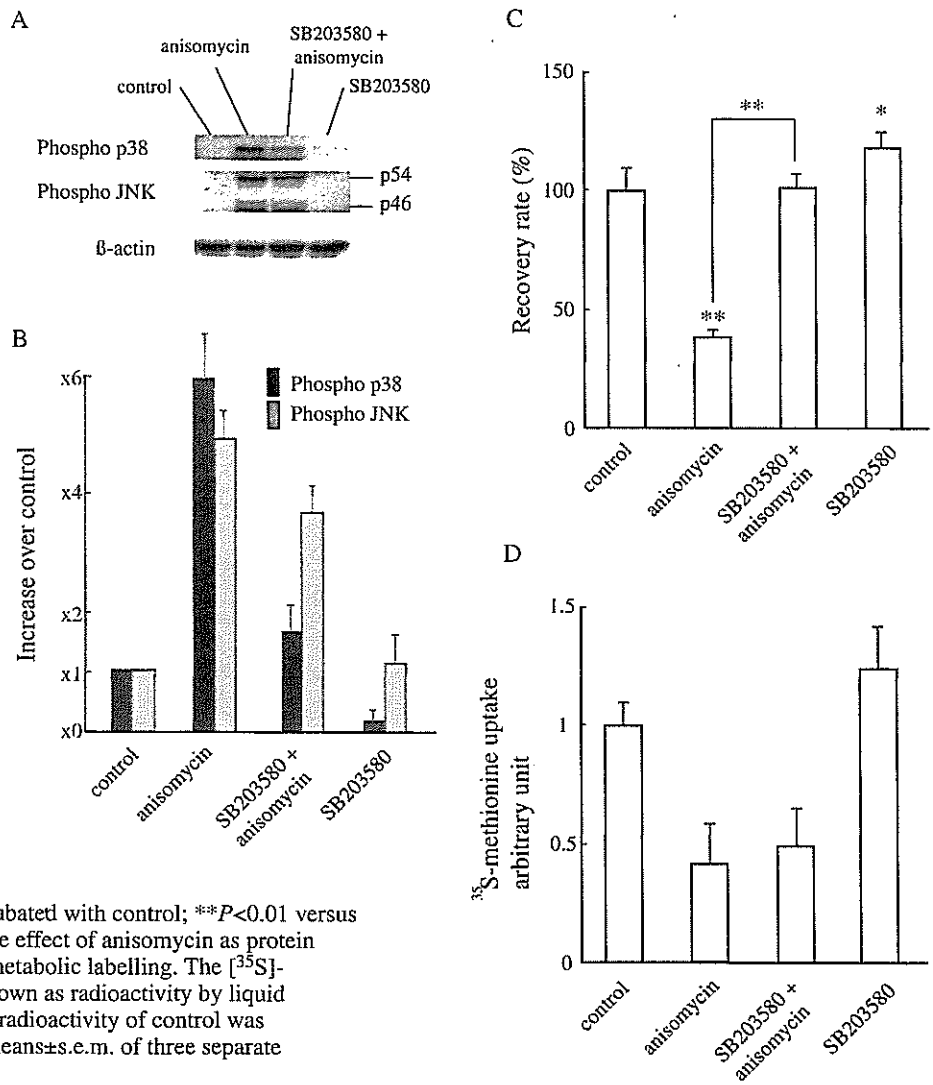

Fig. 5. SB203580 interferes with the effects of anisomycin p38 MAP kinase activity on GJIC. Each treatment group was exposed to 0.02% dimethyl sulfoxide as vehicle alone for 90 minutes (control), anisomycin at 10 μg ml^{-1} for 60 minutes, SB203580 plus anisomycin (pretreatment of SB203580 for 30 minutes, then co-treatment with anisomycin for an additional 60 minutes) or SB203580 alone for 90 minutes. Cells with or without pretreatment with SB203580 at 10 μM were exposed to 10 μg ml^{-1} of anisomycin for 60 minutes. After treatment, samples were prepared as described in Fig. 2B. (A) Typical immunoblot analyses using specific antibodies against phosphorylated forms of p38 MAP kinase, JNK and β-actin as protein-loading control. (B) This result is representative of three experiments, each performed with a different preparation of cells and plotted as the fold activity (mean±s.e.m.) of band density relative to that of control by densitometric analysis. (C) Results are expressed as the percentage (mean±s.e.m.) of RR relative to that of control cells (100%) of at least three separate experiments. *P<0.05 versus cells incubated with control; **P<0.01 versus cells incubated with control. (D) To examine the effect of anisomycin as protein synthesis inhibitor, we used [^{35}S]-methionine metabolic labelling. The [^{35}S]-methionine-incorporated protein levels were shown as radioactivity by liquid scintillation spectrometry. For comparison, the radioactivity of control was arbitrarily set at 1. Results were expressed as means±s.e.m. of three separate experiments.

determine whether SB203580 could inhibit the anisomycin-induced suppression of protein synthesis, we examined the [^{35}S]-methionine contents of total cell lysates and found that SB203580 was not able to restore the level of protein synthesis to the control levels (Fig. 5D). Because the addition of SB203580 appeared to maintain the RR completely (Fig. 5C), it is most likely that the effect of anisomycin on GJIC was not dependent on the inhibition of protein synthesis.

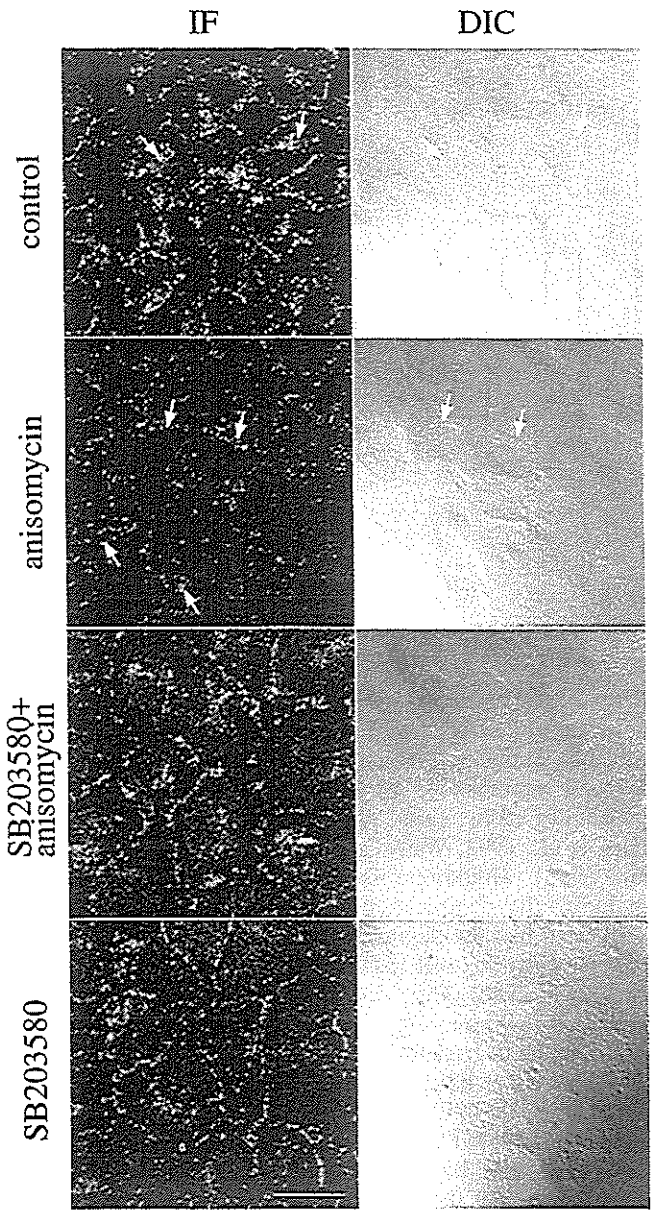

Fig. 6. Anisomycin introduced redistribution of Cx43 and gap-junction plaques. Cx43 was visualized as green spots by indirect immunofluorescence using FITC-labelled secondary antibody. Two sets of quadruple photographs are shown containing immunofluorescence images (IF) and Nomarski differential interference contrast images (DIC) of the same fields. These are typical images of each treatment group. Each treatment group was exposed to 0.02% dimethyl sulfoxide as vehicle alone for 90 minutes (control), anisomycin at 10 μg ml^{-1} for 60 minutes, SB203580 plus anisomycin (pretreatment of SB203580 for 30 minutes, then co-treatment with anisomycin for an additional 60 minutes) or SB203580 alone for 90 minutes. Cytoplasmic staining for Cx43 was also observed (indicated by white arrows). All images in each panel are of the same magnification. Scale bar, 20 μm.

The relationship between p38 MAP kinase phosphorylation/activation and the cellular distribution of Cx43 was assessed by indirect immunofluorescence with monoclonal antibodies in a confocal laser-scanning microscope. Cellular regions containing Cx43 protein molecules were readily identified as a series of brightly stained punctate maculae at the borders of unstimulated cells but significant quantities were located elsewhere (e.g. in a few small compartments adjacent to the nucleus – see the arrows in Fig. 6). By 60 minutes, there was much less Cx43 at most cell borders. These observations are consistent with the profile of anisomycin-induced GJIC loss as judged by FRAP assay results; moreover, the fact that Cx43 protein could still be detected close to cell nuclei after the addition of anisomycin seems to indicate that the anisomycin-induced decreases in GJIC were mostly a result of the loss of Cx43 molecules from cell borders, as opposed to losses from elsewhere in the cell. It is interesting that, as might have been predicted on the basis of our FRAP results, most of the losses of Cx43 molecules from the cell border regions detected in anisomycin-treated WB-F344 cells were not apparent in their SB203580-pretreated counterparts (Fig. 6).

Whole-cell lysates were prepared from cells exposed to SB203580 for 30 minutes before being incubated in the presence or absence of anisomycin. Equal amounts of protein (20 μg) were then extracted from each cell lysate and subjected to SDS-PAGE, immunoblotting and densitometric analyses (Fig. 7A,B). The cells that had been incubated with anisomycin for 60 minutes and, as a result, had lost half their capacity for GJIC turned out to have significantly reduced P1+P2 and P0 levels (Fig. 4). By contrast, cells exposed to 10 μM SB203580 before their anisomycin treatment seemed to lose very little of their P1 and P2. As expected, the P1 and P2 levels in cells exposed to SB203580 alone were virtually the same as those in the appropriate controls. Interestingly, pretreatment of cells with SB203580 did not seem to prevent anisomycin-induced loss of P0, despite their P1+P2 level appearing to be much the same in the presence and absence of anisomycin. We further analysed phosphorylation levels of Cx43 by [^{32}P]-orthophosphate metabolic labelling (Fig. 7C). Incorporated [^{32}P]-phosphates measured as relative radioactivity were augmented, despite the apparent decrease of phosphorylated forms of Cx43 at 60 minutes after anisomycin treatment. This implies that a Cx43 molecule incorporated more phosphates after anisomycin treatment than the untreated control. This phosphorylation augmentation could be almost completely inhibited by the addition of SB203580 (Fig. 7C), indicating that the excess phosphorylation caused by anisomycin is specific to activation of p38 MAP kinase.

Discussion

To resolve the issue of whether p38 MAP kinase is involved in the post-translational regulation of GJIC, experiments were designed to examine whether anisomycin, an activator of p38 MAP kinase and an inhibitor to protein synthesis, could modulate GJIC in a diploid, non-tumorigenic rat liver epithelial cell line. We found that incubation with anisomycin led to marked reductions in GJIC in WB-F344 cells and that

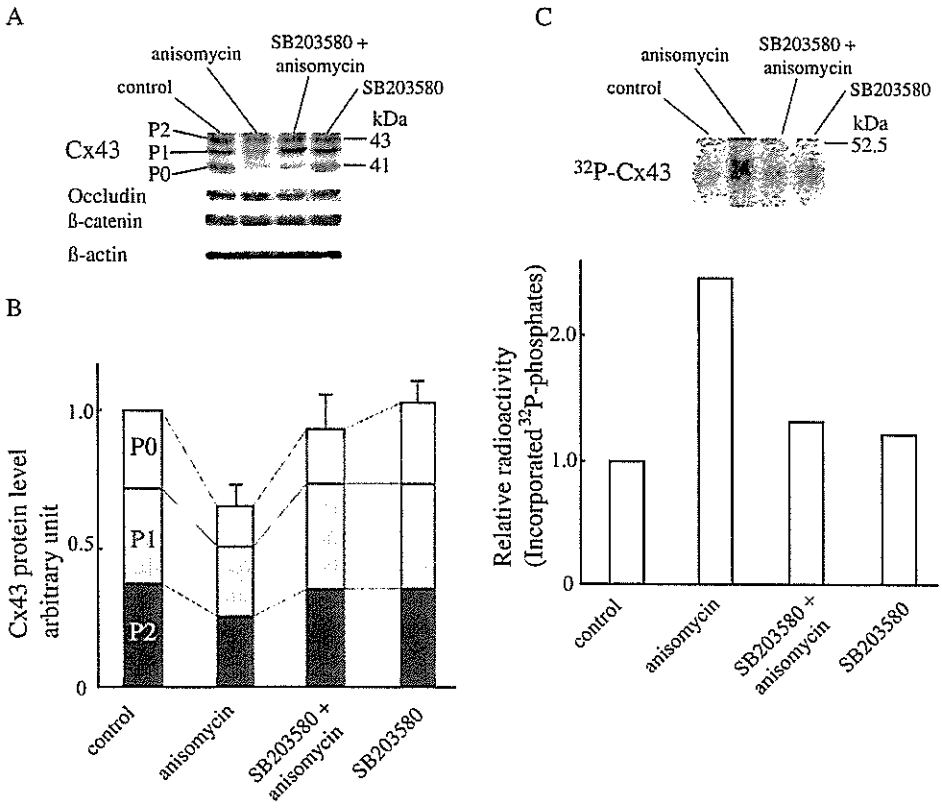

Fig. 7. Western blot analysis of Cx43 protein expression in cells treated with anisomycin and/or SB203580. Each treatment group was exposed to 0.02% dimethyl sulfoxide as vehicle alone for 90 minutes (control), anisomycin at 10 μg ml^{-1} for 60 minutes, SB203580 plus anisomycin (pretreatment of SB203580 for 30 minutes, then co-treatment with anisomycin for an additional 60 minutes) or SB203580 alone for 90 minutes. (A) A typical western blot. Whole-cell extracts (20 μg per lane) were probed with an antibody against Cx43 or against occludin, β-catenin as reference proteins, and against β-actin as a control for protein loading. (B) The relative band intensities of P1, P2 and P0 of Cx43. (C) Autoradiograph of [^{32}P]-orthophosphate labelled Cx43 and its densitometric analysis on an SDS-PAGE gel. Results are from one representative experiment of two separate experiments. To assess each sample, the total value of control radiation was arbitrarily set at 1.

this reduction was accompanied by decreases of the phosphorylated Cx43 protein moieties with which WB-F344 cells are usually associated. The most obvious change involved significant reductions in the levels of the P1 and P2 forms of Cx43. These reductions were reflected in significant losses of Cx43 protein at cellular borders. Such findings are especially interesting in the light of suggestions by previous workers that activation of the ERK signalling pathway leads to hyperphosphorylation of Cx43 and that this in turn leads to reductions in GJIC (Hossain et al., 1998a; Hossain et al., 1999b; Kanemitsu and Lau, 1993; Warn-Cramer et al., 1998; Warn-Cramer et al., 1996).

We reported that GJIC levels are greatly reduced in human primary cultured cells by losses of phosphorylated Cx43 moieties (Ogawa et al., 2001). In the present study, we noted that the absolute levels of phosphorylated Cx43 molecules that we could detect were always significantly lower in anisomycin-treated cells whose GJIC levels had been reduced. This might mean that the decreases in GJIC that we observe in such circumstances are the result of decreases in intracellular levels of phosphorylated Cx43 moieties. Current understanding of gap junction assembly, stability and turnover is that the post-translational phosphorylation of Cx43, as shown by overall changes in species migration on SDS gels, is essential for the functioning of gap junction channels (Elvira et al., 1993; Hossain et al., 1998b; Musil et al., 1990). We therefore believe that there is an additional cause of GJIC disruption in WB-F344 cells: the rapid depletion of phosphorylated Cx43 by anisomycin and the subsequent selective regional losses of Cx43 moieties from cell borders. We found that anisomycin treatment could activate Cx43 phosphorylation and this effect was completely inhibited by the pretreatment with SB203580 (Fig. 7C). This result indicated that the anisomycin-induced activation of MAP kinase actually enhanced phosphorylation of Cx43, although it reduced the total amount of Cx43 protein as well as those of P1 and P2. This might indicate the possibility of increased phosphorylation per Cx43 molecule (Lau et al., 1992; Warn-Cramer et al., 1998; Warn-Cramer et al., 1996), although this conclusion needs further study, including the identification of phosphorylated sites. It has been suggested that the degradation of Cx43 depends on increased phosphorylation level of Cx43 (Girão and Pereira, 2003; Guan and Ruch, 1996). Thus, our interpretation of the present result is that MAP-kinase-activated Cx43 phosphorylation might promote the degradation of Cx43.

We found, as have several other groups (Barros et al., 1997; Cano et al., 1994; Cano and Mahadevan, 1995; Hazzalin et al., 1998; Kyriakis et al., 1994), that anisomycin treatment can lead to activation of both p38 MAP kinase and JNK, and that it almost certainly does so by increasing their phosphorylation levels and hence their capacity for enzymatic action. However, we also demonstrated that anisomycin-induced disruption of GJIC was completely blocked in cells pretreated with 10 μM SB203580 (a concentration that had virtually no effect on the anisomycin-induced phosphorylation of JNK). Given these observations, it seems unlikely that the JNK pathway will prove to play a significant role in the anisomycin-induced disruption of GJIC. Thus, even though anisomycin appears to be capable of provoking the phosphorylation – and hence activation – of JNK, it might well be that its ability to inhibit GJIC is due almost entirely to its ability to activate p38 MAP kinase.

In this study, we used a very high concentration (10 μg ml^{-1}) of anisomycin, primarily because this level was maximally

effective as a GJIC inhibitor in WB-F344 cells (Fig. 2B). We were aware that anisomycin might also act as a translational inhibitor at such concentrations. A previous study (Mahadevan and Edwards, 1991) has shown that relatively low concentrations of anisomycin (around 25-50 ng ml^{-1}; so-called subinhibitory levels) can selectively activate the p38 MAP kinase without inhibiting protein synthesis. In our study, however, even a lower concentration of anisomycin (10 ng ml^{-1}) appeared to have an ability to inhibit protein synthesis, but this concentration could not activate p38 MAP kinase (Fig. 2B, Fig. 3C). This discrepancy might be due to the different cell lines used in the studies. In any event, GJIC could be maintained at the control level by SB203580 pretreatment without recovery of protein synthesis (Fig. 5D), indicating that the effect of anisomycin on GJIC was not dependent on the inhibition of protein synthesis. Our conclusion gained further support from our observation that SB203580 pretreatment of the cells appeared to be capable of preventing anisomycin-induced losses of the P1 or P2 (but not P0) forms of Cx43. Moreover, both before and after treatment in our experiments, we checked the effects on the intracellular levels of ZO-1, occludin, E-cadherin and β-catenin as reference proteins, which have short half-lives like that of Cx43. We did not detect changes in the levels of these reference proteins in any anisomycin treatment experiment.

Anisomycin is also a well known inducer of apoptosis in other cell lines (Polverino and Patterson, 1997; Stadheim and Kucera, 2002). Furthermore, the up- or downregulation of GJIC has been reported in the apoptotic process (Wilson et al., 2000). However, in our experiment, at least up to 120 minutes, anisomycin did not induce apoptosis in WB-F344 cells (data not shown).

A key finding of our present study is that pretreatment of anisomycin-exposed WB-F344 cells with SB203580 appeared to inhibit both the redistribution of Cx43 derivatives and to ameliorate or prevent the disruption of GJIC that anisomycin would otherwise have provoked. It is also important that the protection against GJIC disruption afforded by SB203580 pretreatment was, for all intents and purposes, complete. Given that SB203580 is reputed to be a highly specific inhibitor of p38 MAP kinase (Cuenda et al., 1995; Tong et al., 1997), it seems likely that the most important single event in the anisomycin-induced disruption of GJIC involves its ability to activate this particular kinase. It remains uncertain whether our interpretation will turn out to be an oversimplification, if only because WB-F344 cells pretreated with SB203580 appear to experience virtually no disruption of GJIC under circumstances in which the inhibition of p38 MAP kinase by SB203580 is not complete. Moreover, western blotting analysis revealed that SB203580 was capable of inhibiting JNK and that inhibition of p38 MAP kinase was incomplete. These observations are in accordance with a report that SB203580 is capable of inhibiting JNK when used at relatively high concentrations (Clerk and Sugden, 1998) and others that SB203580 only appears to exert its inhibitory effect on specific isoforms of p38 MAP kinase (Cuenda et al., 1995; Lee et al., 1994). Suggestions that the p38 MAP kinase and JNK pathways engage in cross talk in response to anisomycin might also be relevant (Töröcsik and Szeberényi, 2000). We are currently conducting additional experiments in the hope of obtaining a more thorough understanding of the mechanisms involved in GJIC inhibition by the p38 MAP kinase pathway.

We thank Baxter Limited Renal Division for their support in conducting this study. This study was supported in part by Grants-in-Aid for Scientific Research from the Ministry of Education, Science, Sports and Culture of Japan, and for Cancer Research from the Ministry of Health and Welfare of Japan, and by a grant from the Smoking Research Foundation. We thank E. Suzaki (Department of Histology and Cell Biology, Hiroshima University School of Medicine, Hiroshima, Japan) and K. Yamashita (Department of Anatomy and Developmental Biology, Hiroshima University School of Medicine, Hiroshima, Japan) for helpful advice.

References

Barros, L. F., Young, M., Saklatvala, J. and Baldwin, S. A. (1997). Evidence of two mechanisms for the activation of the glucose transporter GLUT1 by anisomycin: p38(MAP kinase) activation and protein synthesis inhibition in mammalian cells. *J. Physiol.* **504**, 517-525.

Berthoud, V. M., Rook, M. B., Traub, O., Hertzberg, E. L. and Sáez, J. C. (1993). On the mechanisms of cell uncoupling induced by a tumor promoter phorbol ester in clone 9 cells, a rat liver epithelial cell line. *Eur. J. Cell Biol.* **62**, 384-396.

Beyer, E. C., Paul, D. L. and Goodenough, D. A. (1987). Connexin43: a protein from rat heart homologous to a gap junction protein from liver. *J. Cell Biol.* **105**, 2621-2629.

Cano, E., Hazzalin, C. A. and Mahadevan, L. C. (1994). Anisomycin-activated protein kinases p45 and p55 but not mitogen-activated protein kinases ERK-1 and -2 are implicated in the induction of c-Fos and c-Jun. *Mol. Cell Biol.* **14**, 7352-7362.

Cano, E. and Mahadevan, L. C. (1995). Parallel signal processing among mammalian MAPKs. *Trends Biochem. Sci.* **20**, 117-122.

Cho, J. H., Cho, S. D., Hu, H., Kim, S. H., Lee, S. K., Lee, Y. S. and Kang, K. S. (2002). The roles of ERK1/2 and p38 MAP kinases in the preventive mechanisms of mushroom *Phellinus linteus* against the inhibition of gap junctional intercellular communication by hydrogen peroxide. *Carcinogenesis* **23**, 1163-1169.

Clerk, A. and Sugden, P. H. (1998). The p38-MAPK inhibitor, SB203580, inhibits cardiac stress-activated protein kinases/c-Jun N-terminal kinases (SAPKs/JNKs). *FEBS Lett.* **426**, 93-96.

Cuenda, A., Rouse, J., Doza, Y. N., Meier, R., Cohen, P., Gallagher, T. F., Young, P. R. and Lee, J. C. (1995). SB 203580 is a specific inhibitor of a MAP kinase homologue which is stimulated by cellular stresses and interleukin-1. *FEBS Lett.* **364**, 229-233.

Dupont, E., el Aoumari, A., Fromaget, C., Briand, J. P. and Gros, D. (1991). Affinity purification of a rat-brain junctional protein, connexin 43. *Eur. J. Biochem.* **200**, 263-270.

Elvira, M., Díez, J. A., Wang, K. K. and Villalobo, A. (1993). Phosphorylation of connexin-32 by protein kinase C prevents its proteolysis by mu-calpain and m-calpain. *J. Biol. Chem.* **268**, 14294-14300.

Girão, H. and Pereira, P. (2003). Phosphorylation of connexin 43 acts as a stimuli for proteasome-dependent degradation of the protein in lens epithelial cells. *Mol. Vis.* **9**, 24-30.

Guan, X. and Ruch, R. J. (1996). Gap junction endocytosis and lysosomal degradation of connexin43-P2 in WB-F344 rat liver epithelial cells treated with DDT and lindane. *Carcinogenesis* **17**, 1791-1798.

Hazzalin, C. A., le Panse, R., Cano, E. and Mahadevan, L. C. (1998). Anisomycin selectively desensitizes signalling components involved in stress kinase activation and Fos and Jun induction. *Mol. Cell Biol.* **18**, 1844-1854.

Helliwell, P. A., Richardson, M., Affleck, J. and Kellett, G. L. (2000). Regulation of GLUT5, GLUT2 and intestinal brush-border fructose absorption by the extracellular signal-regulated kinase, p38 mitogen-activated kinase and phosphatidylinositol 3-kinase intracellular signalling pathways: implications for adaptation to diabetes. *Biochem. J.* **350**, 163-169.

Hii, C. S., Ferrante, A., Edwards, Y. S., Huang, Z. H., Hartfield, P. J., Rathjen, D. A., Poulos, A. and Murray, A. W. (1995a). Activation of mitogen-activated protein kinase by arachidonic acid in rat liver epithelial WB cells by a protein kinase C-dependent mechanism. *J. Biol. Chem.* **270**, 4201-4204.

Hii, C. S., Ferrante, A., Schmidt, S., Rathjen, D. A., Robinson, B. S., Poulos, A. and Murray, A. W. (1995b). Inhibition of gap junctional communication by polyunsaturated fatty acids in WB cells: evidence that connexin 43 is not hyperphosphorylated. *Carcinogenesis* **16**, 1505-1511.

Hossain, M. Z., Ao, P. and Boynton, A. L. (1998a). Platelet-derived growth

factor-induced disruption of gap junctional communication and phosphorylation of connexin43 involves protein kinase C and mitogen-activated protein kinase. *J. Cell Physiol.* **176**, 332-341.

Hossain, M. Z., Ao, P. and Boynton, A. L. (1998b). Rapid disruption of gap junctional communication and phosphorylation of connexin43 by platelet-derived growth factor in T51B rat liver epithelial cells expressing platelet-derived growth factor receptor. *J. Cell Physiol.* **174**, 66-77.

Hossain, M. Z., Jagdale, A. B., Ao, P. and Boynton, A. L. (1999a). Mitogen-activated protein kinase and phosphorylation of connexin43 are not sufficient for the disruption of gap junctional communication by platelet-derived growth factor and tetradecanoylphorbol acetate. *J. Cell Physiol.* **179**, 87-96.

Hossain, M. Z., Jagdale, A. B., Ao, P., Kazlauskas, A. and Boynton, A. L. (1999b). Disruption of gap junctional communication by the platelet-derived growth factor is mediated via multiple signaling pathways. *J. Biol. Chem.* **274**, 10489-10496.

Kanemitsu, M. Y. and Lau, A. F. (1993). Epidermal growth factor stimulates the disruption of gap junctional communication and connexin43 phosphorylation independent of 12-O-tetradecanoylphorbol 13-acetate-sensitive protein kinase C: the possible involvement of mitogen-activated protein kinase. *Mol. Biol. Cell* **4**, 837-848.

Kyriakis, J. M., Banerjee, P., Nikolakaki, E., Dai, T., Rubie, E. A., Ahmad, M. F., Avruch, J. and Woodgett, J. R. (1994). The stress-activated protein kinase subfamily of c-Jun kinases. *Nature* **369**, 156-160.

Laird, D. W., Castillo, M. and Kasprzak, L. (1995). Gap junction turnover, intracellular trafficking, and phosphorylation of connexin43 in brefeldin A-treated rat mammary tumor cells. *J. Cell Biol.* **131**, 1193-1203.

Lau, A. F., Kanemitsu, M. Y., Kurata, W. E., Danesh, S. and Boynton, A. L. (1992). Epidermal growth factor disrupts gap-junctional communication and induces phosphorylation of connexin43 on serine. *Mol. Biol. Cell* **3**, 865-874.

Lee, J. C., Laydon, J. T., McDonnell, P. C., Gallagher, T. F., Kumar, S., Green, D., McNulty, D., Blumenthal, M. J., Heys, J. R., Landvatter, S. W. et al. (1994). A protein kinase involved in the regulation of inflammatory cytokine biosynthesis. *Nature* **372**, 739-746.

Loewenstein, W. R. (1990). Cell-to-cell communication and the control of growth. *Am. Rev. Respir. Dis.* **142**, S48-S53.

Mahadevan, L. C. and Edwards, D. R. (1991). Signalling and superinduction. *Nature* **349**, 747-748.

Matesic, D. F., Rupp, H. L., Bonney, W. J., Ruch, R. J. and Trosko, J. E. (1994). Changes in gap-junction permeability, phosphorylation, and number mediated by phorbol ester and non-phorbol-ester tumor promoters in rat liver epithelial cells. *Mol. Carcinog.* **10**, 226-236.

Minden, A. and Karin, M. (1997). Regulation and function of the JNK subgroup of MAP kinases. *Biochim. Biophys. Acta* **1333**, F85-F104.

Musil, L. S., Cunningham, B. A., Edelman, G. M. and Goodenough, D. A. (1990). Differential phosphorylation of the gap junction protein connexin43 in junctional communication-competent and -deficient cell lines. *J. Cell Biol.* **111**, 2077-2088.

Musil, L. S. and Goodenough, D. A. (1991). Biochemical analysis of connexin43 intracellular transport, phosphorylation, and assembly into gap junctional plaques. *J. Cell Biol.* **115**, 1357-1374.

Musil, L. S. and Goodenough, D. A. (1993). Multisubunit assembly of an integral plasma membrane channel protein, gap junction connexin43, occurs after exit from the ER. *Cell* **74**, 1065-1077.

Ogawa, T., Hayashi, T., Kyoizumi, S., Ito, T., Trosko, J. E. and Yorioka, N. (1999). Up-regulation of gap junctional intercellular communication by hexamethylene bisacetamide in cultured human peritoneal mesothelial cells. *Lab. Invest.* **79**, 1511-1520.

Ogawa, T., Hayashi, T., Yorioka, N., Kyoizumi, S. and Trosko, J. E. (2001). Hexamethylene bisacetamide protects peritoneal mesothelial cells from glucose. *Kidney Int.* **60**, 996-1008.

Polontchouk, L., Ebelt, B., Jackels, M. and Dhein, S. (2002). Chronic effects of endothelin 1 and angiotensin II on gap junctions and intercellular communication in cardiac cells. *FASEB J.* **16**, 87-89.

Polverino, A. J. and Patterson, S. D. (1997). Selective activation of caspases during apoptotic induction in HL-60 cells. Effects of a tetrapeptide inhibitor. *J. Biol. Chem.* **272**, 7013-7021.

Ruch, R. J., Trosko, J. E. and Madhukar, B. V. (2001). Inhibition of connexin43 gap junctional intercellular communication by TPA requires ERK activation. *J. Cell Biochem.* **83**, 163-169.

Seger, R. and Krebs, E. G. (1995). The MAPK signaling cascade. *FASEB J.* **9**, 726-735.

Stadheim, T. A. and Kucera, G. L. (2002). c-Jun N-terminal kinase/stress-activated protein kinase (JNK/SAPK) is required for mitoxantrone- and anisomycin-induced apoptosis in HL-60 cells. *Leukocyte Res.* **26**, 55-65.

Tong, L., Pav, S., White, D. M., Rogers, S., Crane, K. M., Cywin, C. L., Brown, M. L. and Pargellis, C. A. (1997). A highly specific inhibitor of human p38 MAP kinase binds in the ATP pocket. *Nat. Struct. Biol.* **4**, 311-316.

Töröcsik, B. and Szeberényi, J. (2000). Anisomycin uses multiple mechanisms to stimulate mitogen-activated protein kinases and gene expression and to inhibit neuronal differentiation in PC12 phaeochromocytoma cells. *Eur. J. Neurosci.* **12**, 527-532.

Trosko, J. E., Chang, C. C., Wilson, M. R., Upham, B., Hayashi, T. and Wade, M. (2000). Gap junctions and the regulation of cellular functions of stem cells during development and differentiation. *Methods* **20**, 245-264.

Trosko, J. E. and Ruch, R. J. (1998). Cell-cell communication in carcinogenesis. *Front. Biosci.* **3**, 208-236.

Tsao, M. S., Smith, J. D., Nelson, K. G. and Grisham, J. W. (1984). A diploid epithelial cell line from normal adult rat liver with phenotypic properties of 'oval' cells. *Exp. Cell Res.* **154**, 38-52.

Wade, M. H., Trosko, J. E. and Schindler, M. (1986). A fluorescence photobleaching assay of gap junction-mediated communication between human cells. *Science* **232**, 525-528.

Warn-Cramer, B. J., Cottrell, G. T., Burt, J. M. and Lau, A. F. (1998). Regulation of connexin-43 gap junctional intercellular communication by mitogen-activated protein kinase. *J. Biol. Chem.* **273**, 9188-9196.

Warn-Cramer, B. J., Lampe, P. D., Kurata, W. E., Kanemitsu, M. Y., Loo, L. W., Eckhart, W. and Lau, A. F. (1996). Characterization of the mitogen-activated protein kinase phosphorylation sites on the connexin-43 gap junction protein. *J. Biol. Chem.* **271**, 3779-3786.

Wilson, M. R., Close, T. W. and Trosko, J. E. (2000). Cell population dynamics (apoptosis, mitosis, and cell-cell communication) during disruption of homeostasis. *Exp. Cell Res.* **254**, 257-268.

RADIATION RESEARCH 161, 290–298 (2004)
0033-7587/04 $15.00

Decreases in Percentages of Naïve CD4 and CD8 T Cells and Increases in Percentages of Memory CD8 T-Cell Subsets in the Peripheral Blood Lymphocyte Populations of A-Bomb Survivors

Mika Yamaoka,[a] Yoichiro Kusunoki,[a,1] Fumiyoshi Kasagi,[b] Tomonori Hayashi,[a] Kei Nakachi[a] and Seishi Kyoizumi[a]

Departments of [a] Radiobiology/Molecular Epidemiology and [b] Epidemiology, Radiation Effects Research Foundation, Hiroshima, Japan

Yamaoka, M., Kusunoki, Y., Kasagi, F., Hayashi, T., Nakachi, K. and Kyoizumi, S. Decreases in Percentages of Naïve CD4 and CD8 T Cells and Increases in Percentages of Memory CD8 T-Cell Subsets in the Peripheral Blood Lymphocyte Populations of A-Bomb Survivors. *Radiat. Res.* 161, 290–298 (2004).

Our previous studies have revealed a clear dose-dependent decrease in the percentage of naïve CD4 T cells that are phenotypically CD45RA$^+$ in PBL among A-bomb survivors. However, whether there is a similar radiation effect on CD8 T cells has remained undetermined because of the unreliability of CD45 isoforms as markers of naïve and memory subsets among the CD8 T-cell population. In the present study, we used double labeling with CD45RO and CD62L for reliable identification of naïve and memory cell subsets in both CD4 and CD8 T-cell populations among 533 Hiroshima A-bomb survivors. Statistically significant dose-dependent decreases in the percentages of CD45RO$^-$/CD62L$^+$ naïve cells were found in the CD8 T-cell population as well as in the CD4 T-cell population. Furthermore, the percentages of CD45RO$^+$/CD62L$^+$ and CD45RO$^+$/CD62L$^-$ memory T cells were found to increase significantly with increasing radiation dose in the CD8 T-cell population but not in the CD4 T-cell population. These results suggest that the prior A-bomb exposure has induced long-lasting deficits in both naïve CD4 and CD8 T-cell populations along with increased proportions of these particular subsets of the memory CD8 T-cell population. © 2004 by Radiation Research Society

INTRODUCTION

T-cell homeostasis is achieved by the balance between renewal and death among naïve and memory T cells, and maintenance of both naïve and memory T-cell pools is important for the body to protect itself against intrusions by pathogens (*1*). Exposure to radiation is thought to affect T-cell homeostasis, but little is known about the effects of radiation on the naïve and memory T-cell pools and their relationship to disease development (*2–4*), even though increased risks of various diseases including infectious (*5*) and autoimmune diseases (*6*) are still observed among A-bomb survivors. Our study therefore aimed to clarify whether the previous radiation exposure might have brought about a perturbation of T-cell homeostasis involving maintenance of normal-sized pools of both naïve and memory T cells.

Our previous studies clearly indicated that the percentages of CD4 (helper) T cells, especially those of CD45RA$^+$ (naïve) CD4 T cells, decreased in the PBL of A-bomb survivors; the decrease depended on the radiation dose (*3, 7*). The radiation sensitivity of CD4 and CD8 (cytotoxic) T cells *ex vivo* is approximately equal (*8*). In addition, the majority of CD4 and CD8 T cells are produced in the thymus by the same precursor thymocytes, CD4$^+$/CD8$^+$ cells (*9*). Thus it could be assumed that A-bomb radiation would induce similar damage to peripheral naïve CD4 and CD8 T-cell populations and that the recovery of these T-cell populations would be very similar. However, the question still remained as to the long-term effects of radiation on the recovery of naïve CD8 T-cell populations because of the unreliability of expression of CD45 isoform expression for markers of naïve CD8 T-cell populations. Several studies have proven that the CD45RA$^+$ (i.e. CD45RO$^-$) fraction of the CD8 T-cell population contains some cells that do not express the lymph node homing receptor, CD62L (L-selectin), and that these cells exhibit effector T-cell functions (*10–14*). Further indications from these studies are that naïve CD8 T-cell populations the CD45RA$^+$(CD45RO$^-$) cell fraction can be separated precisely by analyzing their CD62L expression status. In the present study, we conducted three-color flow cytometry using a combination of CD8, CD45RO and CD62L monoclonal antibodies (mAbs) to specifically enumerate the naïve and memory CD8 T-cell populations of A-bomb survivors. The percentages of CD45RO$^-$/CD62L$^+$ (naïve) CD8 T cells were found to decrease dose-dependently in the PBL of the survivors, indicating that the naïve T-cell pools are poorly maintained not only in the CD4 but also in the CD8 T-cell populations

[1] Address for correspondence: Department of Radiobiology/Molecular Epidemiology, Radiation Effects Research Foundation, 5-2 Hijiyama Park, Minami-ku, Hiroshima, 732-0815 Japan; e-mail: ykusunok@rerf.or.jp.

TABLE 1
Characterization of Study Population

	Age (years)[b]								
	<60		60–69		70–79		80+		
Dose (Gy)	Male	Female	Male	Female	Male	Female	Male	Female	Total
<0.005[a]	11	11	23	16	20	41	12	19	153
0.005–0.5	5	5	10	21	23	28	18	20	130
0.5–1.0	9	6	15	25	23	29	7	12	126
1.0–4.0	13	9	15	21	23	26	5	12	124
Total	38	31	63	83	89	124	42	63	533

[a] Individuals in this dose category were exposed at distances in excess of 3 km from the hypocenter and hence received doses that are functionally equivalent to zero.

[b] Age at the time of the examinations, which were conducted between September 2000 and February 2003.

of A-bomb survivors. Flow cytometry using CD62L marker not only allowed precise detection of naïve T cells but also enabled us to determine the percentages of memory T-cell subpopulations in PBL of A-bomb survivors, demonstrating dose-dependent increases in the percentages of $CD45RO^+/CD62L^+$ and $CD45RO^+/CD62L^-$ memory CD8 T cells.

MATERIALS AND METHODS

Study Population

Blood samples were obtained from individual members of an A-bomb survivor cohort in which 1,280 survivors, distributed almost equally by age, gender and radiation dose, had been selected from Hiroshima participants in the Adult Health Study (AHS) at the Radiation Effects Research Foundation (RERF) in 1992 (*3*). The selected study population consists of Hiroshima survivors who were exposed to significant radiation doses of 0.005 Gy or more because of their location within 2 km of the hypocenter plus a second group whose exposures were at distances in excess of 3 km from the hypocenter and as a result would have received less than 0.005 Gy (i.e. would have been exposed to doses that are indistinguishable from background). The latter group of distally exposed survivors includes the most appropriate controls for all of our studies of the effects of A-bomb radiation exposures, including this one. The estimated radiation doses are based on DS86 with the adjustments that are standard practice at RERF (*15, 16*). Of these individuals, 653 reported for examination between September 2000 and February 2003 (see *Flow Cytometry and Schedule of Measurements* below). We decided to exclude results from 120 of these 653 people who had been diagnosed with cancer from our study. The age, gender and radiation dose of the remaining 533 survivors whose lymphocyte samples were subjected to detailed analysis in our study are listed in Table 1. Blood samples were obtained with the informed consent of the survivors, and PBL were separated by the Ficoll-Hypaque gradient technique (*7*).

In Japan, projects of this type must obtain approval from the appropriate Institutional Ethics Committee prior to the commencement of work. In the case of RERF, the relevant committee at the time this project was carried out was known as the Human Investigation Committee, and its approval was sought and granted before the work was started.

Monoclonal Antibodies (mAbs)

FITC-labeled anti-CD4, biotin-labeled anti-CD4, PerCP-labeled anti-CD4, biotin-labeled anti-CD8, PerCP-labeled anti-CD8, phycoerythrin (PE)-labeled anti-CD8, PE-labeled anti-CD3, PerCP-labeled anti-CD3, FITC-labeled anti-CD57, FITC-labeled anti-TCRαβ, and PE-labeled anti-CD62L mAbs were purchased from BD PharMingen (San Diego, CA). PE-labeled anti-CD45RA mAb and FITC-labeled anti-CD45RO mAb were obtained from Coulter Immunotech (Marseille, France) and Caltag Laboratories (Burlingame, CA), respectively.

Flow Cytometry and Schedule of Measurements

Analytical flow cytometry was conducted in a FACScan machine (BD Biosciences, San Jose, CA). Between September 2000 and February 2003, expression of CD45RO and CD62L was analyzed using a combination of FITC-labeled anti-CD45RO, PE-labeled anti-CD62L, and PerCP-labeled anti-CD4 or PerCP-labeled anti-CD8 mAbs. $CD45RO^-/CD62L^+$, $CD45RO^+/CD62L^+$, $CD45RO^+/CD62L^-$ and $CD45RO^-/CD62L^-$ cell fractions in CD4 and CD8 T-cell populations were determined as shown in Fig. 1. Note that we used only bright CD8 expression to identify CD8 T cells to exclude NK cells, which are dully CD8 positive. The percentages of CD45RA-positive naïve and CD45RA-negative memory CD4 T cells in the PBL fractions were measured between October 1992 and March 1995 (*3*). Analyses of the expression of CD45RA in the CD8 T-cell subset involved staining mononuclear cell fractions with FITC-labeled anti-TCRαβ mAb and PE-labeled anti-CD45RA mAb, and with biotin-labeled anti-CD8 mAb sandwiched by streptavidin-RED670 (Gibco BRL, Rockville, MD); the CD45RA expression was determined for the CD8 and TCRαβ double-positive fraction of the survivors' PBL between October 1992 and March 1995. From April 1997 to April 1999, the expression of CD57 in the CD8 T-cell subsets was analyzed using a combination of PE-labeled anti-CD3, PerCP-labeled anti-CD8, and FITC-labeled anti-CD57mAbs; the CD57 expression was determined for the CD3 and CD8 double-positive fraction. The expression of CD28 in the CD8 T-cell subset was analyzed using a combination of PerCP-labeled anti-CD3, PE-labeled anti-CD8, and FITC-labeled anti-CD28mAbs, and the CD28 expression was determined for the CD3 and CD8 double-positive fraction from May 1999 to April 2001. In every measurement, approximately 20,000 cells were analyzed.

Data Analysis

We used a set of data obtained from individuals whose PBL samples were subjected to examinations of CD45RO and CD62L expression to describe the T-cell subpopulations of all 533 A-bomb survivors. Associations of the percentage of each T-cell subpopulation (*percentage*) with age at the time of examination (*age*), gender and radiation dose (*dose*) were analyzed based on the following multiple regression model (*17*), assuming that the percentage of each T-cell subpopulation was related to each explanatory variable in an exponential manner:

$$\log(percentage) = \alpha + \beta_1 age + \beta_2 gender + \beta_3 dose,$$

where

$$gender = \begin{cases} 0 & \text{for male} \quad \text{and} \\ 1 & \text{for female} \end{cases}$$

TABLE 2
Regression Coefficients for Variables Related to the Percentages of CD4 and CD8 T-Cell Subpopulations Expressing Different CD45 Isoforms in PBL among A-Bomb Survivors[a]

Duration of measurements	T-cell subpopulation	Effects			
		Intercept α	Age (10 years)[b] β_1	Gender[c] β_2	Dose (Gy)[d] β_3
September 2000 to February 2003	CD4				
	$CD45RO^-$	4.61	−0.260	0.034	−0.083
			$P = 0.0001$**	$P = 0.56$	$P = 0.036$*
	$CD45RO^+$	3.43	−0.025	0.084	−0.002
			$P = 0.057$	$P = 0.0006$**	$P = 0.92$
	CD8				
	$CD45RO^-$	2.45	−0.098	0.102	−0.063
			$P = 0.0008$**	$P = 0.064$	$P = 0.098$
	$CD45RO^+$	1.98	0.027	−0.077	0.074
			$P = 0.27$	$P = 0.091$	$P = 0.013$*
October 1992 to March 1995	CD4[e]				
	$CD45RA^+$	3.84	−0.124	0.035	−0.054
			$P = 0.0001$**	$P = 0.34$	$P = 0.034$*
	$CD45RA^-$	2.94	0.007	0.65	−0.016
			$P = 0.63$	$P = 0.014$*	$P = 0.35$
	CD8[f]				
	$CD45RA^+$	2.77	−0.065	0.006	0.004
			$P = 0.0053$**	$P = 0.88$	$P = 0.88$
	$CD45RA^-$	1.04	0.022	−0.182	0.043
			$P = 0.49$	$P = 0.0018$**	$P = 0.28$

[a] Regression coefficients of percentage T cells for age, gender and dose were obtained using the following formula: *Percentage T cells* = $\alpha + \beta_1 \times age + \beta_2 \times gender + \beta_3 \times dose$.
[b] Effects of age were estimated for 10-year intervals.
[c] Gender = 0 for male and = 1 for female.
[d] Effects of dose were estimated for 1 Gy.
[e] Results for a total of 723 A-bomb survivors have been reported in ref. (*3*), and those for 497 survivors whose data are available for both the current (2000–2003) and previous (1992–1995) studies are presented here.
[f] Results for 497 survivors whose data are available for both the current and previous studies are presented here.
* $P < 0.05$, ** $P < 0.01$.

RESULTS

Three-Color Flow Cytometry Involving CD62L Expression Revealed Effects of A-Bomb Radiation on Naïve CD8 T-Cell Population

Although a dose-dependent decrease in the percentage of naïve CD4 T cells that were enumerated with the $CD45RA^+$ phenotype has been observed repeatedly among A-bomb survivor populations (*3, 7*), radiation effects on naïve CD8 T-cell populations remained to be investigated. Table 2 summarizes the results of CD45RO expression analyses for a total of 533 A-bomb survivors who were examined between September 2000 and February 2003, along with the results of CD45RA expression analyses that were obtained from previous examinations (October 1992 to March 1995). We found high correlations between the current and previous examinations. The correlation coefficients (r) between the percentages of $CD45RO^-$ (current) and $CD45RA^+$ (previous) subsets in CD4 and CD8 T-cell populations were 0.85 ($P = 0.0001$) and 0.68 ($P = 0.0001$), respectively. Between the percentages of $CD45RO^+$ (current) and $CD45RA^-$ (previous) subsets in CD4 and CD8 T-cell populations, r was 0.75 ($P = 0.0001$) and 0.64 ($P = 0.0001$), respectively. This suggested that it would be reasonable to compare the effects of age, gender and radiation dose on these T-cell subsets in the previous and current examinations. As for CD4 T-cell populations, the effects of age, gender and radiation dose on $CD45RO^-$ and $CD45RO^+$ subsets appeared to be virtually in accord with those effects on $CD45RA^+$ and $CD45RA^-$ subsets. There appeared to be a significant effect of radiation on $CD45RO^+$ CD8 T cells in the current examination but not on the counterpart $CD45RA^-$ CD8 T cells in the previous study. At any rate, significant dose-dependent reductions in the percentages of $CD45RO^-$ and $CD45RA^+$ subsets containing naïve cells were apparent for the CD4 but not CD8 T-cell populations of the survivors, probably due to a substantial fraction of memory CD8 T cells included in the $CD45RO^-$ and $CD45RA^+$ subsets (*10, 18, 19*).

In the present study, we intended to discriminate naïve and memory cells in the $CD45RO^-$ subset by using CD62L as the third marker. Figure 1 shows representative flow cytometry patterns that were obtained from two typical male and female survivors who were relatively young and old. It is clear that the $CD45RO^-$ fraction of CD4 T-cell populations consists mostly of $CD62L^+$ cells, whereas there are

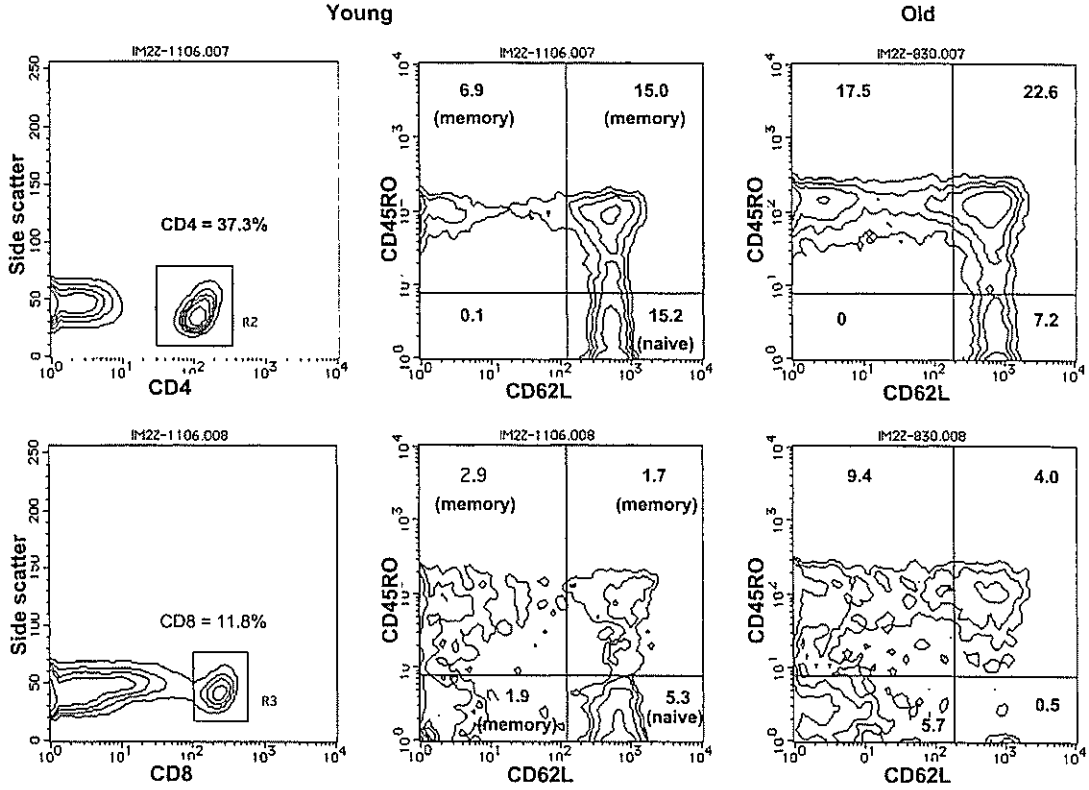

FIG. 1. Flow cytometry patterns of peripheral blood CD4 (upper panel) and CD8 (lower panel) T cells of typical A-bomb survivors who were relatively young (unexposed 58-year-old male, left and center columns) and old (unexposed 93-year-old female, right column), respectively. Peripheral blood mononuclear cells (about 2×10^5) were stained with FITC-labeled anti-CD62L mAb, PE-labeled anti-CD45RO mAb, and PerCP-labeled anti-CD4 mAb (upper panel) or PerCP-labeled anti-CD8 mAb (lower panel). The number in each quadrant indicates the percentage of cells in PBL.

substantial numbers of $CD62L^-$ cells in the $CD45RO^-$ fraction of CD8 T-cell populations. Although there were some individuals who had significant fractions of $CD45RO^-/CD62L^-$ cells in their CD4 T-cell populations, we did not obtain any evidence that A-bomb radiation had affected this minor T-cell subset in any obvious way (data not shown). The $CD45RO^+$ fractions of both CD4 and CD8 T-cell populations can also be divided into $CD62L^+$ and $CD62L^-$ subpopulations. Figure 2 depicts the age and dose trends for the percentage of $CD45RO^-/CD62L^+$ (naïve) cells in CD4 and CD8 T-cell populations. In the CD4 T-cell populations, the percentage of $CD45RO^-/CD62L^+$ (naïve) cells decreased significantly with increased age (25% per 10-year increment, $P = 0.0001$) or radiation dose (9% per gray, $P = 0.034$), almost concordant with that of $CD45RA^+$ or $CD45RO^-$ cells (also see Table 2). As had been expected, the decrease in the percentage of $CD45RO^-/CD62L^+$ (naïve) CD8 T cells was also statistically significant, i.e. a 35% decrease with a 10-year increment of age ($P = 0.0001$) and an 8% decrease per gray ($P = 0.031$). These results clearly indicate that the history of radiation exposure has generated a long-lasting reduction of naïve cell pools in both the CD4 and CD8 T-cell populations among A-bomb survivors.

Dose-Dependent Increases in the Percentages of Memory CD8 T-Cell Subsets

The percentage of $CD45RO^+$ CD8 memory T cells appeared to increase significantly with radiation dose (Table 2). This was not obvious in the measurement with CD45RA, which was used as a naïve/memory marker. To describe the memory T-cell subsets in this study, we determined two distinct $CD62L^+$ and $CD62L^-$ compartments in $CD45RO^+$ cells in both CD4 and CD8 T-cell populations, along with an additional $CD62L^-$ compartment in the $CD45RO^-$ CD8 T-cell population (Fig. 1). It has been reported that memory T cells in the $CD62L^+$ compartment have an increased potential to proliferate in response to recall antigens *in vitro* and a greater capacity to persist *in vivo* than memory T cells in the $CD62L^-$ compartment (*20, 21*). For CD4 but not CD8 T-cell populations, the percentages of $CD45RO^+/CD62L^+$ memory T cells in PBL were found to decrease significantly with increasing age of the A-bomb survivors (Fig. 3 and Table 3). We also found dose-dependent increases in the percentages of $CD45RO^+/CD62L^+$ CD8 T cells (12% increase per gray, $P = 0.0055$) and $CD45RO^+/CD62L^-$ CD8 T cells (8% increase per gray, $P = 0.034$), which were not found for the $CD45RO^+/$

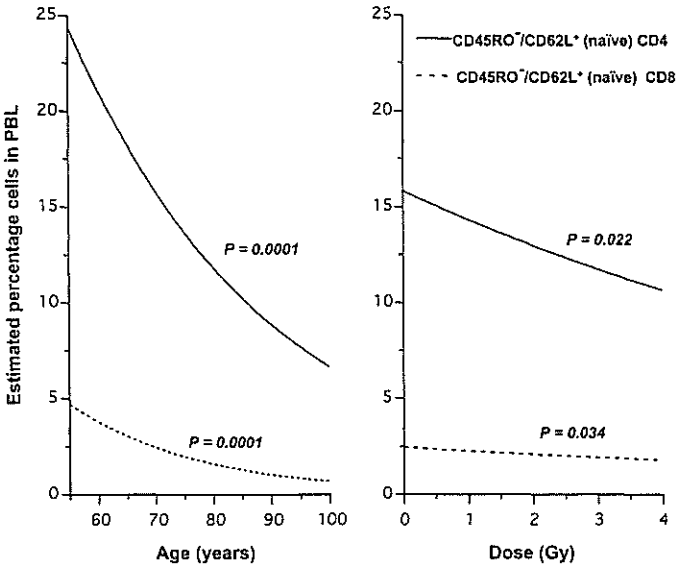

FIG. 2. Estimated radiation dose responses in the percentages of naïve ($CD45RO^-/CD62L^+$) CD4 and CD8 T cells in PBL among 533 A-bomb survivors. The values were adjusted to those of unexposed males or 70-year-old males and plotted as a function of age (left panel) or radiation dose (right panel), respectively, according to the formula described in the Materials and Methods.

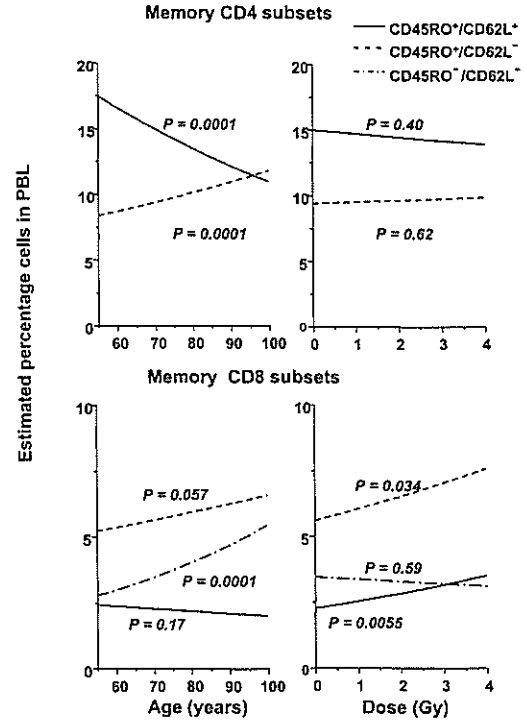

FIG. 3. Estimated radiation dose responses in the percentages of memory CD4 (upper panel) and CD8 (lower panel) T-cell subsets in PBL among 533 A-bomb survivors. The values were adjusted to those of unexposed males or 70-year-old males and plotted as a function of age (left panels) or radiation dose (right panels), respectively, according to the formula described in the Materials and Methods.

$CD62L^+$ or $CD45RO^+/CD62L^-$ CD4 T cells among the same survivors. There was no effect of dose on $CD45RO^-/CD62L^-$ cells in CD8 T-cell populations. These results indicate that the history of radiation exposure has dose-dependently caused increases in subsets ($CD45RO^+/CD62L^+$ and $CD45RO^+/CD62L^-$) of memory CD8 T cells among A-bomb survivors.

Increased Percentages of $CD45RO^+/CD62L^+$ or $CD45RO^+/CD62L^-$ CD8 T Cells by Radiation Exposure may not be Restricted to$CD28^-$ or $CD57^+$ T Cells

Other studies have reported that clonal expansion of a subset of CD8 T cells, such as $CD28^-$ or $CD57^+$, occurred frequently in older individuals (*22–25*). To test whether the increased percentage of $CD45RO^+/CD62L^+$ or $CD45RO^+/CD62L^-$ CD8 T cells that we observed among the survivors was associated with expansion of CD28-negative or CD57-positive cell populations, we analyzed the effects of age, gender and dose on the percentages of $CD28^-$ and $CD57^+$ CD8 T cells and examined the correlations among $CD28^-$, $CD57^+$, $CD45RO^+/CD62L^+$, and $CD45RO^+/CD62L^-$ CD8 T cells (Table 4). The percentages of $CD28^-$ and $CD57^+$ CD8 T cells were much less correlated with those of $CD45RO^+/CD62L^+$ CD8 T cells ($r = 0.18$ and 0.22, respectively) than those of $CD45RO^+/CD62L^-$ CD8 T cells ($r = 0.62$ and 0.60, respectively). This could indicate that expansion of $CD45RO^+/CD62L^-$ CD8 T cells is associated with increased proportions of $CD28^-$ or $CD57^+$ CD8 T cells. However, no significant effect of A-bomb radiation on $CD28^-$ or $CD57^+$ CD8 T cells was found, although there did appear to be a remarkable increase with age in the percentage of these subsets. Thus it is implied that the increased percentages of $CD45RO^+/CD62L^+$ and $CD45RO^+/CD62L^-$ CD8 T cells with increased radiation dose may not be largely due to increases in the percentages of $CD28^-$ and $CD57^+$ CD8 T cells.

DISCUSSION

Our present findings clearly indicate that radiation exposure has reduced the size of naïve cell pools not only in CD4 T-cell populations but also in the other major T-cell subset, CD8, among A-bomb survivors. One of the most plausible explanations for this is that the reduction in the size of naïve T-cell pools could have resulted from an insufficient supply of new T cells from the thymus since the majority of the naïve T cells develop in the thymus. Recently, it has been reported that the numbers of recent thymic emigrant cells can be determined in T-cell populations by detecting T lymphocytes that contain T-cell receptor-rearrangement excision circles (TRECs), which are circular DNA molecules generated in thymocytes during the T-cell receptor gene rearrangement process in the thymus (*26*). It has also been reported that significantly fewer CD4 T cells containing TRECs are currently demonstrable in bone marrow transplantation patients who were exposed to whole-body irradiation more than 20 years ago (*27*). Thus it is

TABLE 3
Regression Coefficients for Variables Related to the Percentages of CD4 and CD8 T-Cell Subpopulations Expressing Different Levels of CD62L in PBL among A-Bomb Survivors[a]

T-cell subpopulation	Effects			
	Intercept α	Age (10 years)[b] β_1	Gender[c] β_2	Dose (Gy)[d] β_3
CD4				
$CD45RO^-/CD62L^+$	4.79	−0.290	0.022	−0.099
		$P = 0.0001$**	$P = 0.72$	$P = 0.022$*
$CD45RO^+/CD62L^+$	3.43	−0.104	0.096	−0.019
		$P = 0.0001$**	$P = 0.0037$**	$P = 0.40$
$CD45RO^+/CD62L^-$	1.71	0.076	0.070	0.012
		$P = 0.0001$**	$P = 0.046$*	$P = 0.62$
CD8				
$CD45RO^-/CD62L^+$	3.92	−0.432	0.170	−0.081
		$P = 0.0001$**	$P = 0.0020$**	$P = 0.034$*
$CD45RO^+/CD62L^+$	1.11	−0.042	0.025	0.109
		$P = 0.17$	$P = 0.66$	$P = 0.0055$**
$CD45RO^+/CD62L^-$	1.37	0.052	−0.116	0.075
		$P = 0.057$	$P = 0.025$*	$P = 0.034$*
$CD45RO^-/CD62L^-$	0.188	0.151	−0.007	−0.027
		$P = 0.0001$**	$P = 0.93$	$P = 0.59$

[a] Regression coefficients of percentage T cells for age, gender and dose were obtained using the following formula: *Percentage T cells* = $\alpha + \beta_1 \times age + \beta_2 \times gender + \beta_3 \times dose$.
[b] Effects of age were estimated for 10-year intervals.
[c] Gender = 0 for male and 1 for female.
[d] Effects of dose were estimated for 1 Gy.
* $P < 0.05$, ** $P < 0.01$.

expected that a similar reduction in the number of recent thymic emigrant cells would be observed among A-bomb survivor populations. Therefore, we recently started measuring the numbers of recent thymic emigrant cells that can be detected in both the CD4 and CD8 T-cell populations of A-bomb survivors with a view to determining whether a reduced production of new T cells in the thymus is an actual cause of the impaired maintenance of naïve T-cell pools among survivors. Another plausible mechanism is that the reduction of the naïve cell pool size might have resulted from the homeostatic and/or antigenic proliferation of naïve T-cell populations followed by their transfer to memory T-cell pools. We are also planning to analyze the turnover of naïve CD4 T-cell populations by tracking genetically marked murine naïve CD4 T cells after implantation into irradiated mice. Such an experimental model will provide us with valuable information for a precise understanding of what happens when radiation exposure seriously impairs the ability of irradiated hosts to maintain normal-sized naïve CD4 T-cell pools.

In most individuals, CD62L-negative cells are undetectable among $CD45RO^-$ CD4 T-cell populations while $CD45RO^-$ CD8 T-cell populations contain a significant fraction of CD62L-negative cells that are known to exhibit potential effector functions (*10–14*). We found that the percentages of $CD45RO^-/CD62L^-$ CD8 T cells increased with age (Fig. 3, Table 3). Although the meaning of this age dependence is unclear, it is not inconceivable that frequent antigen exposures due to decreased immunocompetence in aged individuals leads to an accumulation of effector T-cell populations.

Recent studies suggest that $CD45RA^-(CD45RO^+)$ memory T cells are heterogeneous in their functions and that they comprise distinct populations (*21, 22, 28–34*). These memory subsets can also be distinguished based on the expression of other surface markers, including CD62L (*21, 30, 32, 33*). In addition to impairment in the maintenance of naïve cell pools, our results also suggest that A-bomb radiation has induced a change in the memory T-cell pools of the survivors' CD8 T-cell populations that involves a dose-dependent increase in the percentage of $CD45RO^+/CD62L^+$ or $CD45RO^+/CD62L^-$ cells. Sallusto *et al.* (*28*) have recently proposed that memory ($CD45RA^-$ and $CD45RO^+$) T cells can be classified into central ($CCR7^+$ and mostly $CD62L^+$) and effector ($CCR7^-$ and mostly $CD62L^-$) memory T cells. These subsets were found to show several differences in their functions (*34*), migration capacities (*28*), proliferation abilities (*21, 22, 32*), telomere lengths (*21*), and T-cell receptor repertoires (*33*). These findings suggest that effector memory T cells are immature compared to central memory T cells (*35*), although it is unclear whether the latter memory subset stems from the former (*33, 36*).

Here we discuss possible reasons that the radiation effect is apparent for both the central and effector CD8 memory T-cell subsets. One possible interpretation is that the entry

TABLE 4
Regression Coefficients for Variables Related to the Percentages of CD28-Negative and CD57-Positive CD8 T-Cell Subpopulations and their Correlations to the Percentages of CD45RO$^+$/CD62L$^+$ and CD45RO$^+$/CD62L$^-$ CD8 T Cells in PBL among A-bomb Survivors[a]

T-cell subpopulation	Effects			
	Intercept α	Age (10 years)[b] β_1	Gender[c] β_2	Dose (Gy) β_3
CD28$^-$	1.23	0.177	−0.072	−0.016
		$P = 0.0001$**	$P = 0.25$	$P = 0.70$
CD57$^+$	1.14	0.103	−0.149	−0.033
		$P = 0.0048$**	$P = 0.027$*	$P = 0.48$

Correlation between	Correlation coefficients (r)
CD28$^-$ and CD45RO$^+$/CD62L$^+$	0.18
	$P = 0.0001$**
CD28$^-$ and CD45RO$^+$/CD62L$^-$	0.62
	$P = 0.0001$**
CD57$^+$ and CD45RO$^+$/CD62L$^+$	0.22
	$P = 0.0001$**
CD57$^+$ and CD45RO$^+$/CD62L$^-$	0.60
	$P = 0.0001$**
CD28$^-$ and CD57$^+$	0.84
	$P = 0.0001$**

[a] Regression coefficients of percentage T cells for age, gender and dose were obtained using the following formula: *Percentage T cells* = $\alpha + \beta_1 \times age + \beta_2 \times gender + \beta_3 \times dose$.
[b] Effects of age were estimated for 10-year intervals.
[c] Gender = 0 for male and = 1 for female.
* $P < 0.05$, ** $P < 0.01$.

of naïve CD8 T cells into the memory T-cell pool is enhanced in A-bomb survivors. Repeated exposure of naïve CD8 T cells to various antigens could have led to accumulation of both central and effector memory T cells. Impaired immunity to persistent infections with viruses such as EBV (*37, 38*), HBV (*5, 39*) and HCV (*40, 41*) in A-bomb survivors might be involved in this accumulation process. Homeostatic proliferation that takes place in the absence of antigen under lymphopenic conditions such as radiation-induced lymphopenia may also have contributed to the enhanced entry of naïve T cells into memory T-cell pools. However, such a possibility may contradict a previous finding, in which a population of mutant stem cells of one A-bomb survivor did not contributed greatly to the maintenance of the survivor's memory T-cell pool after A-bomb exposure (*42*).

Another interpretation is that clonal expansions of a population of memory CD8 T cells have frequently occurred in A-bomb survivors. A recent cytogenetic study on A-bomb survivors has shown that the frequency of clonal chromosome aberrations increased with increasing radiation dose and suggested that about half of the clonal chromosome aberrations may have been derived from clonal expansions of memory T cells (*43*). It has also been found that skewed TCR Vβ repertoires that are possibly associated with clonal expansions can frequently be observed in CD45RA$^-$ memory CD4 T-cell populations of A-bomb survivors, especially in those of older survivors (*44*). Although we have not yet determined the TCR Vβ repertoires in CD8 T-cell populations of the survivors, similar expansions of memory CD8 T cells can be expected among radiation-exposed persons. Nevertheless, the dose-dependent increases in the percentages of CD45RO$^+$/CD62L$^+$ and CD45RO$^+$/CD62L$^-$ memory T cells were apparent for CD8 T-cell populations but not for CD4 T-cell populations, suggesting that clonal expansions frequently occurring in the exposed individuals might not accompany the accumulation of memory T cells.

In contrast to the dose-dependent increases in the percentages of CD45RO$^+$/CD62L$^+$ and CD45RO$^+$/CD62L$^-$ CD8 T cells, there was no significant effect of radiation on these subsets of memory CD4 T cells in the present study. Although it has been established that no antigenic stimulation is required for either the CD4 or CD8 T-cell populations to maintain immunological memory, the ways in which the memory T-cell pools maintain their sizes are likely to be somewhat different for CD4 and CD8 T-cell populations. Thus, for example, homeostatic proliferation of memory CD8 T cells is accomplished by IL7 and IL15, whereas unknown factors other than those cytokines are probably involved in that of memory CD4 T cells (*45, 46*). Memory CD8 T cells are likely to persist *in vivo* for much longer than memory CD4 T cells (*47*). Furthermore, age-associated reductions in the diversity of TCR repertoire were found to be much more pronounced in memory CD8 populations than memory CD4 populations (*48*). Such differences in the CD4 and CD8 T-cell populations may be associated with the different radiation effects we observed in the CD45RO$^+$/CD62L$^+$ and CD45RO$^+$/CD62L$^-$ subsets of these T-cell populations among A-bomb survivors. The mechanisms by which radiation exposure impairs the ability of humans to maintain T-cell memory remain to be clarified.

ACKNOWLEDGMENTS

The authors would like to thank Mika Yonezawa and Yoko Takemoto for their help with manuscript preparation. The Radiation Effects Research Foundation (RERF), Hiroshima and Nagasaki, is a private nonprofit foundation funded by the Japanese Ministry of Health, Labour and Welfare (MHLW) and the United States Department of Energy (DOE), the latter through the National Academy of Sciences. This publication was based on RERF Research Protocol RP 1-93.

Received: September 3, 2003; accepted: November 13, 2003

REFERENCES

1. A. W. Goldrath and M. J. Bevan, Selecting and maintaining a diverse T-cell repertoire. *Nature* **402**, 255–262 (1999).
2. Y. Kusunoki, S. Kyoizumi, M. Yamaoka, F. Kasagi, K. Kodama and T. Seyama, Decreased proportion of CD4 T cells in the blood of

atomic bomb survivors with myocardial infarction. *Radiat. Res.* **152**, 539–543 (1999); Erratum. *Radiat. Res.* **154**, 119 (2000).

3. Y. Kusunoki, M. Yamaoka, F. Kasagi, T. Hayashi, K. Koyama, K. Kodama, D. G. MacPhee and S. Kyoizumi, T cells of atomic bomb survivors respond poorly to stimulation by *Staphylococcus aureus* toxins *in vitro*: Does this stem from their peripheral lymphocyte populations having a diminished naive CD4 T-cell content? *Radiat. Res.* **158**, 715–724 (2002).
4. T. Hayashi, Y. Kusunoki, M. Hakoda, Y. Morishita, Y. Kubo, M. Maki, F. Kasagi, K. Kodama, D. G. MacPhee and S. Kyoizumi, Radiation dose-dependent increases in inflammatory response markers in A-bomb survivors. *Int. J. Radiat. Biol.* **79**, 129–136 (2003).
5. S. Fujiwara, S. Kusumi, J. Cologne, M. Akahoshi, K. Kodama and H. Yoshizawa, Prevalence of anti-hepatitis C virus antibody and chronic liver disease among atomic bomb survivors. *Radiat. Res.* **154**, 12–19 (2000).
6. S. Nagataki, Y. Shibata, S. Inoue, N. Yokoyama, M. Izumi and K. Shimaoka, Thyroid diseases among atomic bomb survivors in Nagasaki. *J. Am. Med. Assoc.* **272**, 364–370 (1994).
7. Y. Kusunoki, S. Kyoizumi, Y. Hirai, T. Suzuki, E. Nakashima, K. Kodama and T. Seyama, Flow cytometry measurements of subsets of T, B and NK cells in peripheral blood lymphocytes of atomic bomb survivors. *Radiat. Res.* **150**, 227–236 (1998).
8. N. Nakamura, Y. Kusunoki and M. Akiyama, Radiosensitivity of CD4 or CD8 positive human T-lymphocytes by an *in vitro* colony formation assay. *Radiat. Res.* **123**, 224–227 (1990).
9. E. L. Reinherz and S. F. Schlossman, The differentiation and function of human T lymphocytes. *Cell* **19**, 821–827 (1980).
10. R. L. Rabin, M. Roederer, Y. Maldonado, A. Petru and L. A. Herzenberg, Altered representation of naive and memory CD8 T cell subsets in HIV-infected children. *J. Clin. Invest.* **95**, 2054–2060 (1995).
11. L. J. Picker, J. R. Treer, B. Ferguson-Darnell, P. A. Collins, P. R. Bergstresser and L. W. Terstappen, Control of lymphocyte recirculation in man. II. Differential regulation of the cutaneous lymphocyte-associated antigen, a tissue-selective homing receptor for skin-homing T cells. *J. Immunol.* **150**, 1122–1136 (1993).
12. M. Roederer, J. G. Dubs, M. T. Anderson, P. A. Raju and L. A. Herzenberg, CD8 naive T cell counts decrease progressively in HIV-infected adults. *J. Clin. Invest.* **95**, 2061–2066 (1995).
13. J. M. McCune, R. Loftus, D. K. Schmidt, P. Carroll, D. Webster, L. B. Swor-Yim, I. R. Francis, B. H. Gross and R. M. Grant, High prevalence of thymic tissue in adults with human immunodeficiency virus-1 infection. *J. Clin. Invest.* **101**, 2301–2308 (1998).
14. F. F. Fagnoni, R. Vescovini, G. Passeri, G. Bologna, M. Pedrazzoni, G. Lavagetto, A. Casti, C. Franceschi, M. Passeri and P. Sansoni, Shortage of circulating naive $CD8^+$ T cells provides new insights on immunodeficiency in aging. *Blood* **95**, 2860–2868 (2000).
15. D. A. Pierce, D. O. Stram and M. Vaeth, Allowing for random errors in radiation dose estimates for the atomic bomb survivor data. *Radiat. Res.* **123**, 275–284 (1990).
16. D. A. Pierce, Y. Shimizu, D. L. Preston, M. Vaeth and K. Mabuchi, Studies of the mortality of atomic bomb survivors. Report 12, Part I. Cancer: 1950–1990. *Radiat. Res.* **146**, 1–27 (1996).
17. G. Armitage, G. Berry and J. N. S. Matthews, *Statistical Methods in Medical Research.* Blackwell Science, Oxford, 2002.
18. D. Hamann, P. A. Baars, M. H. Rep, B. Hooibrink, S. R. Kerkhof-Garde, M. R. Klein and R. A. van Lier, Phenotypic and functional separation of memory and effector human $CD8^+$ T cells. *J. Exp. Med.* **186**, 1407–1418 (1997).
19. M. R. Wills, A. J. Carmichael, M. P. Weekes, K. Mynard, G. Okecha, R. Hicks and J. G. Sissons, Human virus-specific $CD8^+$ CTL clones revert from CD45ROhigh to CD45RAhigh *in vivo*: CD45RAhigh $CD8^+$ T cells comprise both naive and memory cells. *J. Immunol.* **162**, 7080–7087 (1999).
20. R. J. Hogan, E. J. Usherwood, W. Zhong, A. A. Roberts, R. W. Dutton, A. G. Harmsen and D. L. Woodland, Activated antigen-specific $CD8^+$ T cells persist in the lungs following recovery from respiratory virus infections. *J. Immunol.* **166**, 1813–1822 (2001).
21. R. L. Hengel, V. Thaker, M. V. Pavlick, J. A. Metcalf, G. Dennis, Jr., J. Yang, R. A. Lempicki, I. Sereti and H. C. Lane, Cutting edge: L-selectin (CD62L) expression distinguishes small resting memory $CD4^+$ T cells that preferentially respond to recall antigen. *J. Immunol.* **170**, 28–32 (2003).
22. D. N. Posnett, R. Sinha, S. Kabak and C. Russo, Clonal populations of T cells in normal elderly humans: The T cell equivalent to "benign monoclonal gammapathy". *J. Exp. Med.* **179**, 609–618 (1994).
23. F. F. Fagnoni, R. Vescovini, M. Mazzola, G. Bologna, E. Nigro, G. Lavagetto, C. Franceschi, M. Passeri and P. Sansoni, Expansion of cytotoxic $CD8^+$ $CD28^-$ T cells in healthy ageing people, including centenarians. *Immunology* **88**, 501–507 (1996).
24. J. K. Morley, F. M. Batliwalla, R. Hingorani and P. K. Gregersen, Oligoclonal $CD8^+$ T cells are preferentially expanded in the $CD57^+$ subset. *J. Immunol.* **154**, 6182–6190 (1995).
25. N. Khan, N. Shariff, M. Cobbold, R. Bruton, J. A. Ainsworth, A. J. Sinclair, L. Nayak and P. A. Moss, Cytomegalovirus seropositivity drives the CD8 T cell repertoire toward greater clonality in healthy elderly individuals. *J Immunol.* **169**, 1984–1992 (2002).
26. D. C. Douek, R. D. McFarland, P. H. Keiser, E. A. Gage, J. M. Massey, B. F. Haynes, M. A. Polis, A. T. Haase, M. B. Feinberg and R. A. Koup, Changes in thymic function with age and during the treatment of HIV infection. *Nature* **396**, 690–695 (1998).
27. K. Weinberg, B. R. Blazar, J. E. Wagner, E. Agura, B. J. Hill, M. Smogorzewska, R. A. Koup, M. R. Betts, R. H. Collins and D. C. Douek, Factors affecting thymic function after allogeneic hematopoietic stem cell transplantation. *Blood* **97**, 1458–1466 (2001).
28. F. Sallusto, D. Lenig, R. Forster, M. Lipp and A. Lanzavecchia, Two subsets of memory T lymphocytes with distinct homing potentials and effector functions. *Nature* **401**, 708–712 (1999).
29. L. Lefrancois, Dual personality of memory T cells. *Trends Immunol.* **23**, 226–228 (2002).
30. T. Ohara, K. Koyama, Y. Kusunoki, T. Hayashi, N. Tsuyama, Y. Kubo and S. Kyoizumi, Memory functions and death proneness in three $CD4^+CD45RO^+$ human T cell subsets. *J Immunol.* **169**, 39–48 (2002).
31. L. S. Cauley, T. Cookenham, T. B. Miller, P. S. Adams, K. M. Vignali, D. A. Vignali and D. L. Woodland, Cutting edge: virus-specific $CD4^+$ memory T cells in nonlymphoid tissues express a highly activated phenotype. *J. Immunol.* **169**, 6655–6658 (2002).
32. J. Geginat, A. Lanzavecchia and F. Sallusto, Proliferation and differentiation potential of human $CD8^+$ memory T-cell subsets in response to antigen or homeostatic cytokines. *Blood* **101**, 4260–4266 (2003).
33. V. Baron, C. Bouneaud, A. Cumano, A. Lim, T. P. Arstila, P. Kourilsky, L. Ferradini and C. Pannetier, The repertoires of circulating human $CD8^+$ central and effector memory T cell subsets are largely distinct. *Immunity* **18**, 193–204 (2003).
34. D. Masopust, V. Vezys, A. L. Marzo and L. Lefrancois, Preferential localization of effector memory cells in nonlymphoid tissue. *Science* **291**, 2413–2417 (2001).
35. E. J. Wherry, V. Teichgraber, T. C. Becker, D. Masopust, S. M. Kaech, R. Antia, U. H. von Andrian and R. Ahmed, Lineage relationship and protective immunity of memory CD8 T cell subsets. *Nat. Immunol.* **4**, 225–234 (2003).
36. F. Sallusto and A. Lanzavecchia, Exploring pathways for memory T cell generation. *J. Clin. Invest.* **108**, 805–806 (2001).
37. M. Akiyama, Y. Kusunoki, S. Kyoizumi, K. Ozaki, S. Mizuno and J. B. Cologne, Study of the titers of anti-Epstein-Barr virus antibodies in the sera of atomic bomb survivors. *Radiat. Res.* **133**, 297–302 (1993).
38. Y. Kusunoki, S. Kyoizumi, Y. Fukuda, H. Huang, M. Saito, K. Ozaki, Y. Hirai and M. Akiyama, Immune responses to Epstein-Barr virus in atomic bomb survivors: Study of precursor frequency of cytotoxic lymphocytes and titer levels of anti-Epstein-Barr virus-related antibodies. *Radiat. Res.* **138**, 127–132 (1994).
39. K. Neriishi, S. Akiba, T. Amano, T. Ogino and K. Kodama, Prevalence of hepatitis B surface antigen, hepatitis B e antigen and anti-

body, and antigen subtypes in atomic bomb survivors. *Radiat. Res.* **144**, 215–221 (1995).

40. S. Fujiwara, G. B. Sharp, J. B. Cologne, S. Kusumi, M. Akahoshi, K. Kodama, G. Suzuki and H. Yoshizawa, Prevalence of hepatitis B virus infection among atomic bomb survivors. *Radiat. Res.* **159**, 780–786 (2003).

41. G. B. Sharp, T. Mizuno, J. B. Cologne, T. Fukuhara, S. Fujiwara, S. Tokuoka and K. Mabuchi, Hepatocellular carcinoma among atomic bomb survivors: Significant interaction of radiation with hepatitis C virus infections. *Int. J. Cancer* **103**, 531–537 (2003).

42. Y. Kusunoki, Y. Hirai, M. Hakoda and S. Kyoizumi, Uneven distributions of naive and memory T cells in the CD4 and CD8 T-cell populations derived from a single stem cell in an atomic bomb survivor: Implications for the origins of the memory T-cell pools in adulthood. *Radiat. Res.* **157**, 493–499 (2002).

43. M. Nakano, Y. Kodama, K. Ohtaki, M. Itoh, A. A. Awa, J. Cologne, Y. Kusunoki and N. Nakamura, Estimating the number of hematopoietic or lymphoid stem cells giving rise to clonal chromosome aberrations in blood T lymphocytes. *Radiat. Res.* **161**, 273–281 (2004).

44. Y. Kusunoki, M. Yamaoka, F. Kasagi, T. Hayashi, D. G. MacPhee and S. Kyoizumi, Long-lasting changes in the T-cell receptor V beta repertoires of CD4 memory T-cell populations in the peripheral blood of radiation-exposed people. *Br. J. Haematol.* **122**, 975–984 (2003).

45. T. E. Boursalian and K. Bottomly, Survival of naive CD4 T cells: Roles of restricting versus selecting MHC class II and cytokine milieu. *J. Immunol.* **162**, 3795–3801 (1999).

46. X. Zhang, S. Sun, I. Hwang, D. F. Tough and J. Sprent, Potent and selective stimulation of memory-phenotype $CD8^-$ T cells *in vivo* by IL-15. *Immunity* **8**, 591–599 (1998).

47. D. Homann, L. Teyton and M. B. Oldstone, Differential regulation of antiviral T-cell immunity results in stable $CD8^+$ but declining $CD4^+$ T-cell memory. *Nat. Med.* **7**, 913–919 (2001).

48. A. Wack, A. Cossarizza, S. Heltai, D. Barbieri, S. D'Addato, C. Franceschi, P. Dellabona and G. Casorati, Age-related modifications of the human αβ T cell repertoire due to different clonal expansions in the $CD4^+$ and $CD8^+$ subsets. *Int. Immunol.* **10**, 1281–1288 (1998).

RADIATION RESEARCH 161, 273–281 (2004)
0033-7587/04 $15.00

Estimating the Number of Hematopoietic or Lymphoid Stem Cells Giving Rise to Clonal Chromosome Aberrations in Blood T Lymphocytes

M. Nakano,[a,1] Y. Kodama,[a] K. Ohtaki,[a] M. Itoh,[a] A. A. Awa,[a] J. Cologne,[b] Y. Kusunoki[c] and N. Nakamura[a]

Departments of [a] Genetics, [b] Statistics and [c] Radiobiology/Molecular Epidemiology, Radiation Effects Research Foundation, 5-2 Hijiyama Park, Minami-ku, Hiroshima 732-0815, Japan

Nakano, M., Kodama, Y., Ohtaki, K., Itoh, M., Awa, A. A., Cologne, J., Kusunoki, Y. and Nakamura, N. Estimating the Number of Hematopoietic or Lymphoid Stem Cells Giving Rise to Clonal Chromosome Aberrations in Blood T Lymphocytes. *Radiat. Res.* 161, 273–281 (2004).

Quantifying the proliferative capacity of long-term hematopoietic stem cells in humans is important for bone marrow transplantation and gene therapy. Obtaining appropriate data is difficult, however, because the experimental tools are limited. We hypothesized that tracking clonal descendants originating from hematopoietic stem cells would be possible if we used clonal chromosome aberrations as unique tags of individual hematopoietic stem cells *in vivo*. Using FISH, we screened 500 blood T lymphocytes from each of 513 atomic bomb survivors and detected 96 clones composed of at least three cells with identical aberrations. The number of clones was inversely related to their population size, which we interpreted to mean that the progenitor cells were heterogeneous in the number of progeny that they could produce. The absolute number of progenitor cells contributing to the formation of the observed clones was estimated as about two in an unexposed individual. Further, scrutiny of ten clones revealed that lymphocyte clones could originate roughly equally from hematopoietic stem cells or from mature T lymphocytes, thereby suggesting that the estimated two progenitor cells are shared as one hematopoietic stem cell and one mature T cell. Our model predicts that one out of ten people bears a non-aberrant clone comprising >10% of the total lymphocytes, which indicates that clonal expansions are common and probably are not health-threatening.

INTRODUCTION

Hematopoiesis is the process by which hematopoietic stem cells differentiate into various kinds of blood cells, including lymphocytes. Long-term hematopoietic stem cells have been characterized extensively in animal model systems because they are directly relevant to hematopoietic stem cell transplantation and gene therapy (see refs. *1–3*). For example, human hematopoietic stem cells in adult bone marrow are characterized as $CD34^+$ $Thy\text{-}1^+$ Lin^- $Rh123^{dull}$ (*2*). The frequency of the long-term hematopoietic stem cells among the bone marrow cells is estimated to be 10^{-4} to 10^{-5} (*2*). Studies on the proliferation potential of hematopoietic stem cells indicate that one (or a few) long-term hematopoietic stem cell can reconstitute hematopoiesis in lethally irradiated mice (*4, 5*) and cats (*6*). In larger animals such as rhesus monkeys, single-cell engraftment studies are not possible, but it is suggested that hematopoiesis is polyclonal (*7*). Human data are rare because hematopoietic stem cell assays are limited, but in a few instances, the indication is that single hematopoietic stem cells can reconstitute nearly all of the T-lymphocyte population. For example, in a few patients suffering from hereditary severe combined immune deficiency, the affected gene reverted spontaneously to normal in apparently single committed T-cell progenitors, and the revertants proliferated so as to overcome the T-cell deficiency and greatly improve the clinical condition (*8–10*). These data demonstrate the enormous proliferation capability of single progenitor cells *in vivo* under certain conditions. It remains to be known, however, how the hematopoietic system is constructed and maintained under ordinary conditions and the number of active hematopoietic stem cells involved therein.

During the course of cytogenetic studies to evaluate the radiation dose (biodosimetry) to atomic bomb (A-bomb) survivors, we and others found identical chromosome aberrations in multiple T lymphocytes (in at least three) (*11–14*) or in both T lymphocytes and other hematopoietic cells (*14, 15*). These aberrations are termed clonal chromosome aberrations, because they are derived from single progenitor cells and produced by their large clonal expansions. The aberrations are composed mainly of translocations but occasionally include inversions as well. Clonal aberrations are observed in other radiation-exposed individuals as well (*16–22*). We considered the possibility that such clonal aberrations could serve as unique non-invasive "tags" for examining the gross clonal structure of the human hematopoietic system *in vivo*. Since 100 to 1,000 cells are usually scored for chromosome aberrations in biodosimetric studies, and the total lymphocyte number in the human body is

[1] Address for correspondence: Department of Genetics, Radiation Effects Research Foundation, 5-2 Hijiyama Park, Minami-ku, Hiroshima 732-0815, Japan; e-mail: Mimako_Nakano@rerf.or.jp.